



**Michigan Ion Beam Laboratory**  
FOR SURFACE MODIFICATION AND ANALYSIS

---

**ANNUAL RESEARCH REPORT**

**2012**

Gary S. Was, Director  
Ovidiu Toader, Operations Manager  
Fabian Naab, Engineer

2600 Draper Road  
Department of Nuclear Engineering and Radiological Sciences  
University of Michigan  
Ann Arbor, Michigan 48109-2145  
<http://www.ners.engin.umich.edu/research/mibl/>

Telephone: (734) 936-0166

Fax: (734) 763-4540

## ***The Annual Research Report***

This report summarizes the principal research activities in the Michigan Ion Beam Laboratory during the past calendar year. Eighty-eight researchers conducted thirty-eight projects at MIBL that accounted for over 3300 hours of equipment usage. The programs included participation from researchers at the University, corporate research laboratories, private companies, government laboratories, and other universities across the United States. The extent of participation of the laboratory in these programs ranged from routine surface analysis to ion assisted film formation. Experiments included Rutherford backscattering spectrometry, elastic recoil spectroscopy, nuclear reaction analysis, direct ion implantation, ion beam mixing, ion beam assisted deposition, and radiation damage by proton bombardment. The following pages contain a synopsis of the research conducted in the Michigan Ion Beam Laboratory during the 2011 calendar year.

### ***About the Laboratory***

The Michigan Ion Beam Laboratory for Surface Modification and Analysis was completed in October of 1986. The laboratory was established for the purpose of advancing our understanding of ion-solid interactions by providing up-to-date equipment with unique and extensive facilities to support research at the cutting edge of science. Researchers from the University of Michigan as well as industry and other universities are encouraged to participate in this effort.

The lab houses a 1.7 MV tandem ion accelerator, a 400 kV ion implanter, and an ion beam assisted deposition (IBAD) system. Additional facilities include a vacuum annealing furnace, a surface profilometry system, and a scanning laser surface curvature measurement system. The control of the parameters and the operation of these systems are mostly done by computers and are interconnected through a local area network, allowing off-site monitoring and control.

In 2010, MIBL became a Partner Facility of the Advanced Test Reactor, National Scientific User Facility (ATR-NSUF), at Idaho National Laboratory, providing additional opportunities for researchers across the US to access the capabilities of the laboratory. In its first two years as a Partner Facility, MIBL hosted five ATR projects.

Respectfully submitted,

A handwritten signature in black ink, appearing to read "Gary S. Was". The signature is written in a cursive style with a large initial "G".

Gary S. Was, Director

# **RESEARCH PROJECTS**

# IRRADIATION EFFECTS IN FERRITIC-MARTENSITIC STEELS AT VERY HIGH DOSES

E. M. Beckett, J. P. Wharry, Z. Jiao, G. Yu, G. S. Was

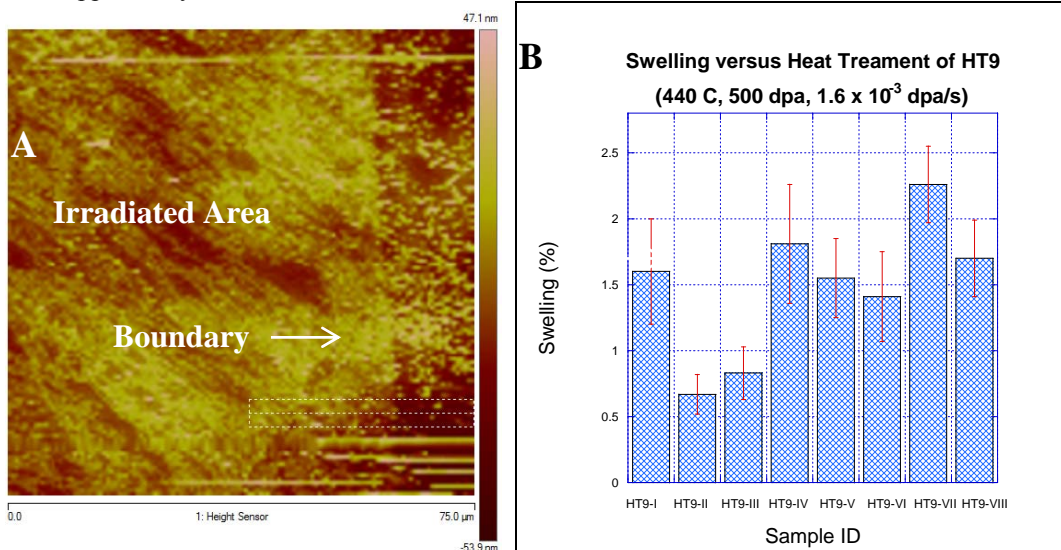
Department of Nuclear Engineering and Radiological Sciences, University of Michigan

This project will study the effects of very high doses of irradiation, up to 500 dpa, in HT9 and other ferritic-martensitic (F-M) steels, in the range of 400-500°C, which is the anticipated operating temperature regime of the TerraPower, LLC traveling wave reactor. Of greatest interest is the microstructural evolution under irradiation, including void swelling, dislocation loop nucleation and growth, and precipitation.

Thus far, work has focused on developing an efficient method for measuring void swelling. Measurement of swelling via transmission electron microscopy (TEM) is time-consuming both in sample preparation and sample analysis. An alternative, macroscopic, method measures bulk swelling via a “step” at the boundary between irradiated and unirradiated regions of the sample. A well-defined step is created by masking a portion of the sample with a stainless steel or tantalum knife blade. The height of the step can be related to bulk swelling. Measurement of the step was performed via atomic force microscopy (AFM). Materials examined in this study included F-M alloy HT9 with eight different heat treatments. Irradiations were performed at 440°C to 500 dpa with 5.0 MeV Fe<sup>++</sup> ions. F-M alloys show swelling resistance that has been shown to be highly dependent on heat treatment. A step was observed in all eight different heat treatments of HT-9, corresponding to swelling between 0.67±0.15 % and 2.26±0.29%.

Future work will include refining sample preparation techniques and step height analysis techniques, which will be used in upcoming irradiations of up to 500 or 600 dpa in order to examine the high dose microstructural evolution.

This work is supported by TerraPower, LLC.



A) Boundary between irradiated and unirradiated area as seen in AFM scan after irradiation to 500 dpa at 440°C. B) Swelling measured by step height method in 8 heat treated samples of HT9

# TRISO-COATED FUEL DURABILITY UNDER EXTREME CONDITIONS

I. Reimanis<sup>1</sup>, D. Butt<sup>2</sup>

Collaborators: <sup>2</sup>John Youngsman, <sup>1</sup>Brian Gorman, Micron Surface Analysis Group, Michigan Ion Beam Laboratory

<sup>1</sup>Metallurgical and Materials Engineering, Colorado School of Mines

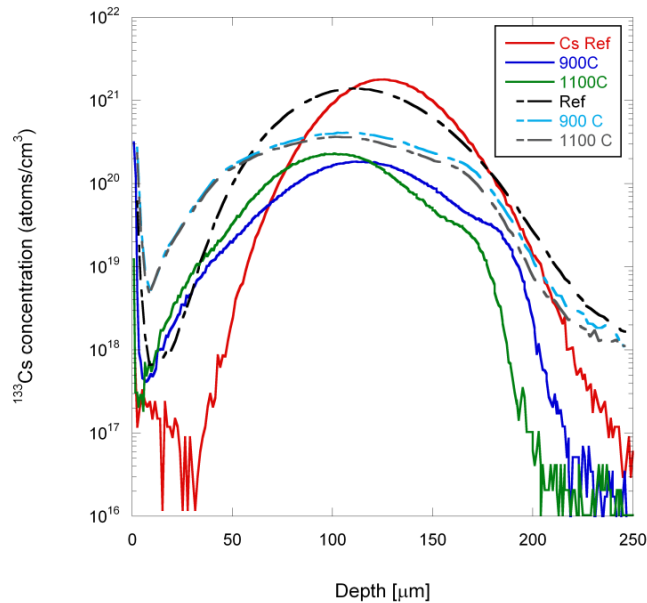
<sup>2</sup>College of Engineering, Boise State University

The current study will examine the effect of CO-CO<sub>2</sub> environments on the oxidation behavior of the SiC layer of a TRISO particle and the resulting change in mechanical performance. Corrosion of the carbide layer can occur in the presence of a number of species produced during reactor fission events. Some of these products are seen to diffuse through the carbide layer. Diffusion studies are used to aid in a thorough understanding of the kinetic behavior of the system.

Presently, the diffusion work consists of ion implanted substrates (accomplished at the Michigan Ion Beam Laboratory) of cesium and palladium that are subjected to various heat treatments with varying dwell time, temperature and atmosphere. Analysis is accomplished with SIMS at the Micron Surface Analysis Lab. Additional analyses of structure is conducted with the TEM, SEM, and XPS instruments that are part of the Boise State Center for Materials Characterization. Mechanical testing is completed at the Colorado School of Mines facility.

Results show improved retention of Cs in the SiC substrate for samples subjected to heat treatments at indicated temperatures for 8 hours. Loss of Cs occurs due to implant damage (solid lines). Recrystallization of the substrates provides for improved retention in the SiC (dashed lines) thus providing better diffusion data.

Research is supported under NEUP Award Number: DE-AC07-05ID14517, Project Number: 09-257.



Composition vs. depth profiles from SIMS analysis for Cs-implanted SiC following various heat treatments.

# ACCELERATOR BASED STUDY OF IRRADIATION CREEP IN PYROLYTIC CARBON USED IN VHTR TRISO FUEL PARTICLES

A. A. Campbell, G. S. Was

Department of Nuclear Engineering and Radiological Sciences, University of Michigan

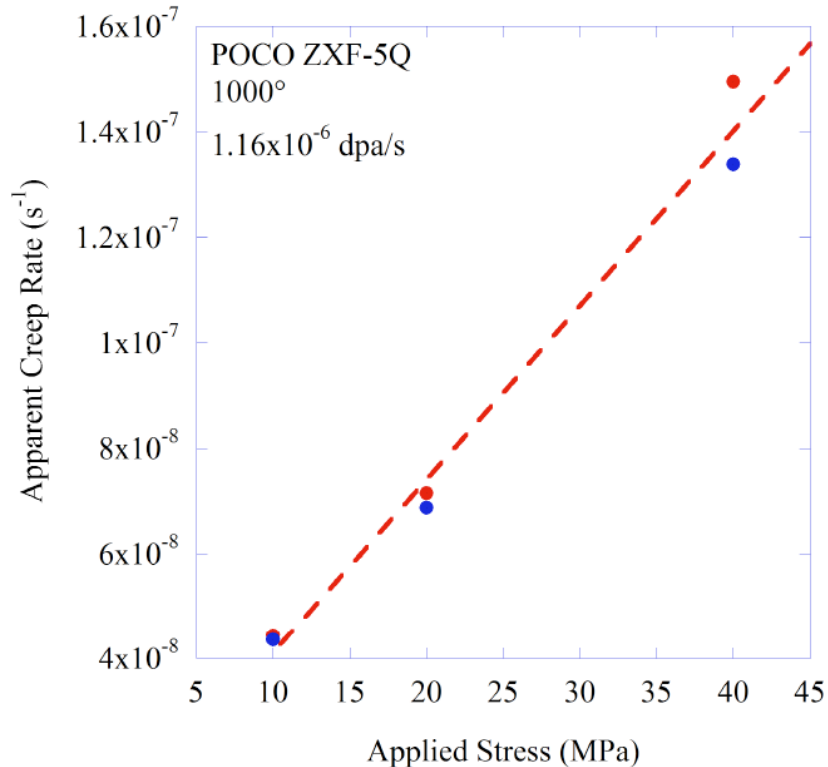
This work has focused on performing proton irradiation induced creep experiments on pyrolytic carbon (PyC). Pyrolytic carbon is the primary coating material for the TRISO fuel particles for the Gen-IV Very High Temperature Reactor (VHTR). Current research is being performed with graphite strips until pyrolytic carbon samples become available.

The most recent irradiation induced creep experiment was performed to determine the effect of applied tensile stress on the creep behavior of graphite. The figure shows a summary of the creep results for three different applied stresses for creep tests conducted with 3MeV protons at 1000°C and at a dose rate of  $\sim 1.15 \times 10^{-7}$  dpa/s. Initial results show that the creep rate follows a linear dependence on the applied tensile stress as follows:

$$\dot{\epsilon}(s^{-1}) = 3.30 \times 10^{-9} \sigma + 8.27 \times 10^{-9}$$

where stress is in MPa.

This work is supported by the Department of Energy under NERI grant DE-FC07-06ID14732.



Apparent creep rate measured by the laser speckle extensometer (red) and by a linear variable differential transducer (blue). The linear fit shown with the red dashed line is calculated for the combined LSE and LVDT values.

# HIGH TEMPERATURE BEHAVIOR OF SILVER IMPLANTED INTO SILICON CARBIDE

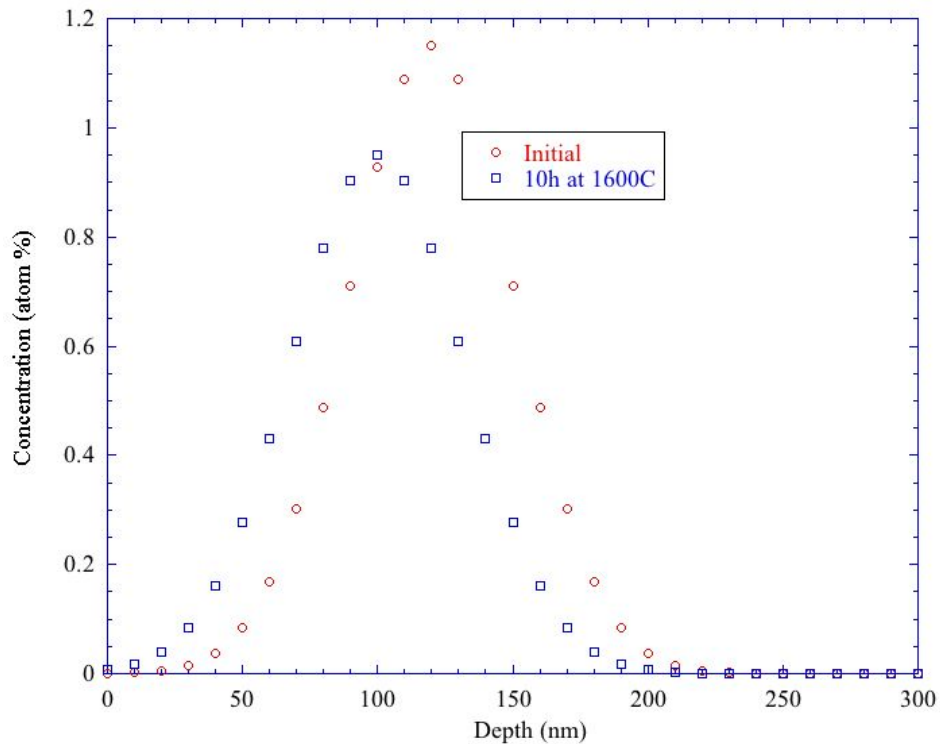
S. Dwaraknath, G.S. Was

Department of Nuclear Engineering and Radiological Sciences, University of Michigan

This work focused on confirming the possibility of a non-Fickian diffusion mechanism for silver (Ag) in silicon carbide (SiC). SiC is the primary fission product barrier in the TRISO fuel design and silver is one of the fission products known to permeate the SiC layer. Previous ion implantation studies of Ag diffusion in SiC have shown significant losses of Ag in the diffusion couple without any broadening of the Gaussian composition profile.

Diffusion couples have been made by direct implantation of silver into SiC samples to a fluence of  $1 \times 10^{16} \text{ atoms/cm}^2$ . Rutherford Backscattering Analysis was used to verify the implantation profile using a 2 MeV  $He^{++}$  ion beam and a backscatter angle of 160 degrees. The results shown in the Figure give the Ag composition profiles following implantation and implantation and annealing at 1600°C for 10 hr. The full width half maxima (FWHM) for the initial and annealed profiles are 72 nm and 75 nm, which are both within the error for RBS, while the integrated concentrations are  $9.27 \times 10^{15} \text{ cm}^{-2}$  and  $7.12 \times 10^{15} \text{ cm}^{-2}$  respectively. The loss of Ag without any apparent broadening can be explained by a non-Fickian diffusion mechanism such as volatilized transport via a network of micro-cracks.

This work is supported by the Department of Energy under NEUP Contract #00103195



Ag composition profiles for ion implanted SiC after implantation and after annealing for 10 hours at 1600°C.

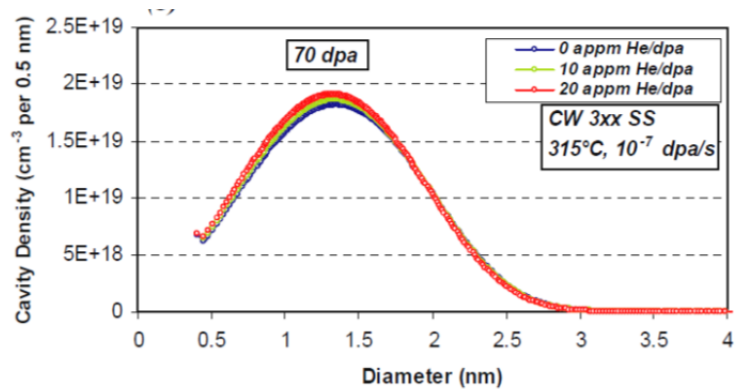
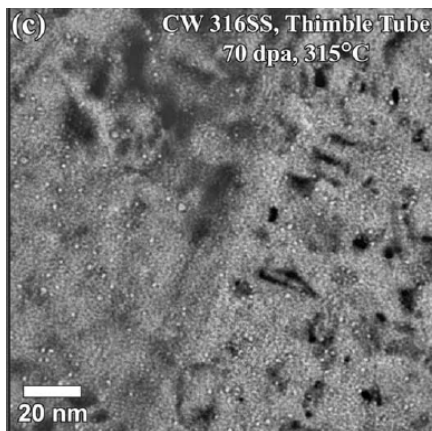
# COMPARISON OF CLUSTER DYNAMICS PREDICTION WITH THE MICROSTRUCTURE OF PROTON IRRADIATED AUSTENITIC STAINLESS STEEL AT 500°C

L. Fournier  
AREVA NP SAS, France

A cluster dynamics model is being developed by AREVA NP SAS for the prediction of the entire microstructure evolution of austenitic stainless steel (SS) under irradiation. The particular features of the model are the description of (i) the creation and evolution of stacking fault tetrahedra (SFT), (ii) the evolution of the Frank loops and network dislocation microstructure, (iii) the influence of helium considering the mean number of helium atoms in cavities.

This model was calibrated against 304L austenitic SS data on Frank loops and SFTs after irradiation in the Bor60 fast reactor at 320°C and  $9.4 \times 10^{-7}$  dpa/s. The predictions of the model have been compared to experimental data from the Ringhals PWR thimble tube CW 316 austenitic stainless steel irradiated at 315°C,  $10^{-7}$  dpa/s, and 20 appm He/dpa. Results were found to be in good agreement.

The objective of this project is to compare the predictions of the model with the microstructure of a proton irradiated austenitic stainless steel at 500°C,  $10^{-5}$  dpa/s; paying a particular attention to void swelling.



TEM micrograph of the Ringhals PWR flux thimble tube irradiated at 70 dpa and 315°C showing a high density of small cavities and cluster dynamics prediction of the cavity density distribution as a function of size.

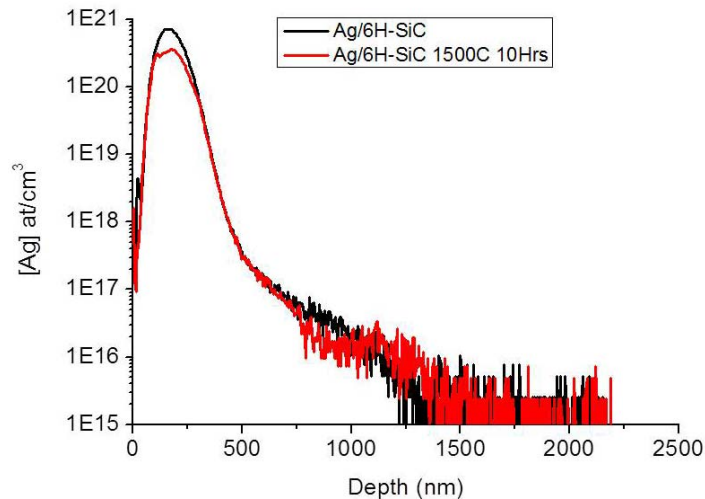
# MICROSTRUCTURAL AND IRRADIATION EFFECTS ON Ag AND Cs DIFFUSION

T. J. Gerczak, T. R. Allen  
Materials Science Program, University of Wisconsin-Madison

Release of Ag and Cs fission products from intact TRISO fuel limits fuel lifetime and creates safety and maintenance concerns in the high temperature gas cooled reactor design. The release mechanisms for Ag and Cs have not been directly observed and are hypothesized to be dominated by short circuit diffusion mechanism. This work aims to understand the release behavior of Ag and Cs through an ion implantation diffusion couple study. Single crystal and polycrystalline SiC substrates have been ion implanted with Ag and Cs through an Advanced Test Reactor National User Facility proposal at the University of Michigan Ion Beam Laboratory.

In the ion implantation diffusion study the Gaussian implantation peak serves as a constant source approximation. After thermal exposure impurity diffusion can be observed by penetration of the diffusing species further into the bulk past the implantation peak. From this redistribution of the implanted species insight on diffusion kinetics can be determined. The change in concentration is being measured by depth profiling using Secondary Ion Mass Spectroscopy (SIMS). Initial samples have been exposed to temperatures 1200-1700C. The preliminary results suggest impurity diffusion is active in the system. This is indicated in the, SIMS depth profile for Ag in single crystal SiC exposed to 1500C for 10 hr, where Ag has diffused past the straggling concentration (Figure). These promising initial results are furthering the study. The role of individual grain boundaries on short circuit impurity diffusion will also be investigated by understanding the penetration distance and segregation of the diffusing species past the implantation peak to specific grain boundaries.

This work is supported by DoE NERI Grant Award No. DE-FC07-07ID14823 and NRC Grant Award NRC-04-07-120 and this research utilized NSF-supported shared facilities at the University of Wisconsin. Part of this research was performed using EMSL, a national scientific user facility sponsored by the Department of Energy's Office of Biological and Environmental Research located at Pacific Northwest National Laboratory (PNNL).



SIMS depth profiles of Ag in single crystal SiC, As-implanted and implanted plus annealed at 1500°C for 10 hr.

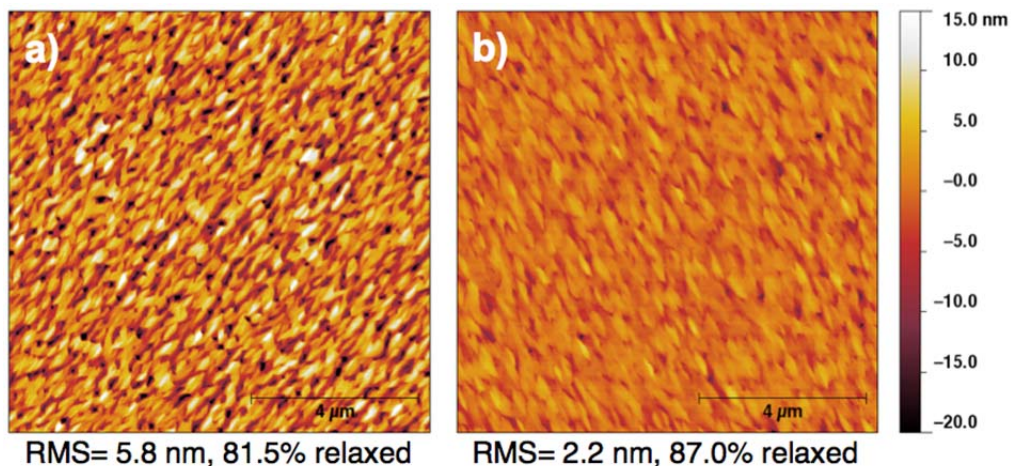
# ENGINEERING STRAIN RELAXATION BY PRE-IMPLANTATION OF SEMICONDUCTOR SUBSTRATES

K.A. Grossklaus, J.M. Millunchick

Department of Materials Science and Engineering, University of Michigan

Recent work has shown that blanket ion implantation of group IV substrates before film growth can result in improved film quality and defect reduction [1]. However, a similar pre-implantation approach has not previously been explored in the III-V semiconductor system. In this work  $\text{Ar}^+$  ion pre-implantation of GaAs substrates has been investigated as a route to engineering film relaxation and defect placement in III-V lattice mismatched heterostructures. GaAs substrates have been implanted with 25 kV or 50 kV Ar ions and followed by the growth of  $\text{In}_x\text{Ga}_{1-x}\text{As}$  films. Atomic force microscope (AFM) characterization of 50, 100, and 1000 nm thick  $\text{InGaAs}$  films grown on ion implanted GaAs substrates shows that they are much smoother than similar films grown on unimplanted substrates (Figure). High resolution x-ray diffraction (HRXRD) analysis of the implanted films also indicates that they are more relaxed in comparison. Transmission electron microscopy (TEM) of film cross sections shows that substrate pre-implantation leads to increased dislocation densities in the  $\text{In}_x\text{Ga}_{1-x}\text{As}$  films and again confirms that pre-implantation results in lower film roughness. Thus by pre-implanting before growth a dislocated and smooth film may be produced. This effect may be exploited to produce a high quality layer for subsequent device growth. By combining pre-implantation with a heterostructure designed to limit threading dislocation propagation, it may be possible to produce a substrate for subsequent device layer growth that is both smooth and free of threading defects. Research examining this combined approach is currently ongoing.

[1] Y. Hsieh, et al., *Appl. Phys. Lett.* **90**, 083507 (2007).



AFM images showing the surfaces of  $\text{In}_{0.25}\text{Ga}_{0.75}\text{As}$  films grown on a) an unimplanted GaAs substrate and b) a 50 kV  $\text{Ar}^+$  ion pre-implanted substrate. The field of view for both images is 10  $\mu\text{m}$ . The RMS roughness and percent relaxation as determined by HRXRD for each sample are given below each image. The film grown on the implanted substrate is both smoother and more relaxed.

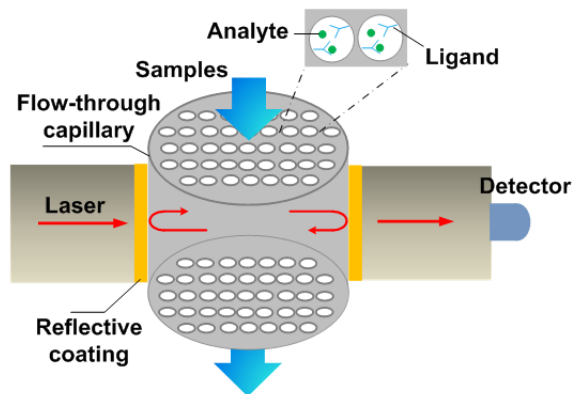
# OPTOFLUIDIC FABRY-PÉROT CAVITY BIOSENSOR WITH INTEGRATED FLOW-THROUGH MICRO/NANO CHANNELS

Y. Guo, H. Li, K. Reddy, X. Fan

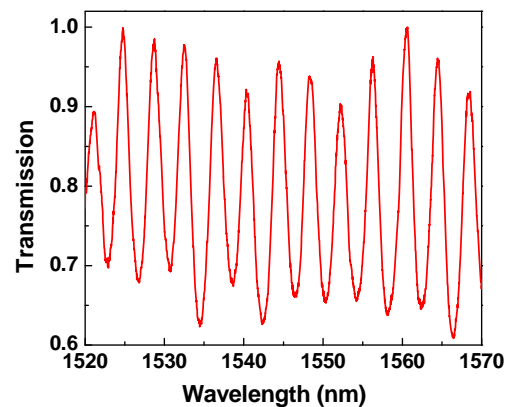
Department of Biomedical Engineering, University of Michigan

Effective integration between label-free sensors and micro-/nano-fluidics is highly desirable for efficient sample delivery to achieve rapid and sensitive detection. However, currently most of the label-free sensors employ the “flow-over” scheme, which relies on the analytes in bulk solution to diffuse to the sensing surface and suffers from mass transport problems. In order to address the inefficient analyte delivery issues, we propose, fabricate, characterize, and demonstrate an optofluidic Fabry-Pérot (FP) cavity sensor with integrated flow-through micro/nanofluidic channels. As illustrated in the Figure (left) the optofluidic FP sensor employs a micro-sized capillary with many built-in micro/nano-sized flow-through holes. When the capillary is placed between two reflectors, a FP cavity forms and detects the analytes binding to the internal surface of the holes. The sensor’s detection resolution depends on the resonance width of the FP cavity.

To get a high-finesse FP resonator, a Bragg mirror structure, that is, multiple alternating pairs consisting of higher-index and lower-index dielectric layers like  $(\text{TiO}_2/\text{SiO}_2)^N$  ( $N$  is the number of alternating pairs), is used as the reflector directly coated on the capillary or on the facet of single-mode fibers. Experimentally, we coated 4 pairs of  $(\text{TiO}_2/\text{SiO}_2)$  layers on the outer surface of the capillary as the reflectors, and measured its transmission spectrum, as shown in the Figure (right). The FP resonance mode has a full-width-at-half-maximum of about 3.1 nm (obtained by Lorentz fitting), corresponding to a Q-factor of 500 (much higher than other flow-through sensors).



Schematic of FP sensor consisting of surface-coated flow-through multihole capillary



Normalized transmission spectrum of the FP sensor using the surface-coated capillary

[1] Guo, Y., Li, H., Reddy, K., Shelar, H. S., Nittoor, V. R., and Fan, X., “Optofluidic Fabry-Pérot Cavity Biosensor with Integrated Flow-Through Micro-/Nanochannels,” *Appl. Phys. Lett.*, 98, 041104 (2011).

# DEVELOPING A MECHANISTIC UNDERSTANDING OF RADIATION TOLERANT MATERIALS

D.T. Hoelzer<sup>1</sup>, P. Duo<sup>1</sup>, G.S. Was<sup>2</sup>, E. Marquis<sup>3</sup>

<sup>1</sup>Oak Ridge National Laboratory

<sup>2</sup>Department of Nuclear Engineering and Radiological Sciences, University of Michigan

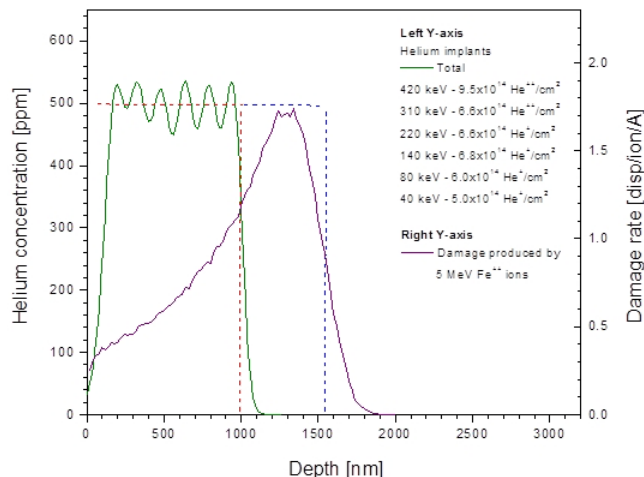
<sup>3</sup>Department of Materials Science and Engineering, University of Michigan

In this work, high dose Fe ion irradiation and He ion implantation experiments were conducted to study the tolerance of the advanced oxide dispersion strengthened (ODS) 14YWT ferritic alloy (Fe-14Cr-3W-0.4Ti-0.3Y<sub>2</sub>O<sub>3</sub> - wt. %) to radiation damage, including the accumulation of He. The 14YWT ferritic alloy contains a high concentration of nano-sized Ti-, Y- and O-enriched clusters (NC) and ultra-fine grains that act as high sink strength for attracting radiation produced point defects, resulting in their recombination, and transmutation products, such as He, to form nano-size bubbles or cavities that prevents He from accumulating on grain boundaries to form large bubbles that cause embrittlement of alloys. The very high internal interfacial area associated with these microstructural features forms the basis of the high sink strength concept. Results obtained from these experiments will help guide further developments in advanced alloys to achieve the radiation tolerance required for future nuclear reactor concepts.

Several Fe ion irradiation and He implantation experiments were conducted on specimens of 14YWT (SM11 heat) during the past year. To study the stability of the NC to irradiation damage, samples were irradiated with 5 MV Fe<sup>2+</sup> ions to 10, 100 and 200 dpa at 200°C using the 1.7 MV Tandem Accelerator. In another set of experiments 14YWT specimens were pre-implanted with 500 appm He at 25°C into the surface of the specimens using the 400 kV Ion Implanter followed by irradiating the specimens with 5 MV Fe<sup>2+</sup> ions to 10 dpa at 200°C and 500°C to study the trapping mechanism of He by the NC. Two polished specimens of 14YWT were used in each experiment. After the experiment was completed, one specimen of 14YWT from each experiment was sent to ORNL for Transmission Electron Microscopy (TEM) analysis and the other specimen was retained at the U. Michigan for Local Electrode Atom Probe (LEAP) analysis. Specimens for TEM analysis are currently being prepared at ORNL using the lift-out Focused Ion Beam (FIB) technique in conjunction with SRIM (Stopping and Range of Ions in Matter) plot (Figure) showing the depth profile of the damage zone produced by Fe<sup>2+</sup> ions and the distribution of He ions. Similar specimen preparation will be performed at the University of Michigan for LEAP analysis.

This research was sponsored by US Department of Energy, Office of Nuclear Energy under Contract DE-AC05-00OR22725 with UT-Battelle, LLC.

SRIM plot showing the He distribution near the surface of the 14YWT specimen and the subsequent damage profile produced from Fe<sup>2+</sup> ion irradiation.



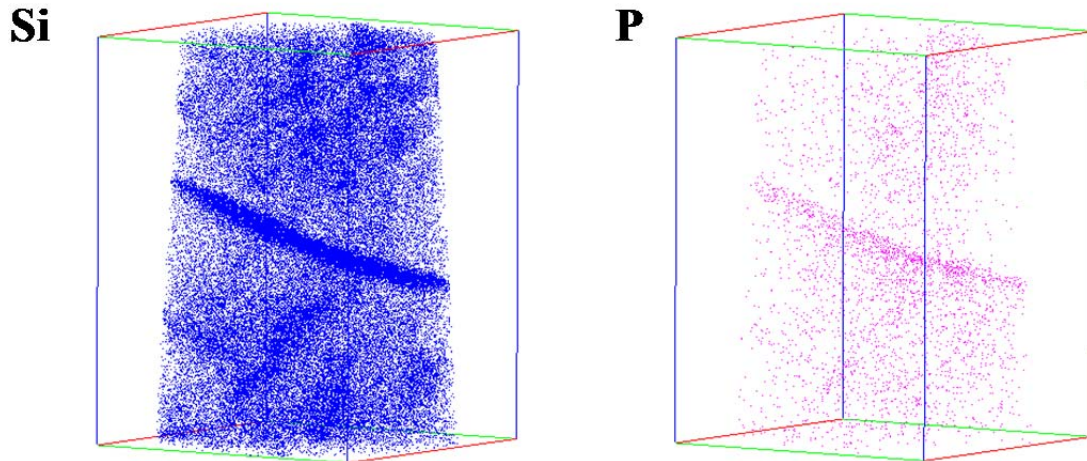
# AGING AND EMBRITTLEMENT OF HIGH FLUENCE STAINLESS STEELS

Z. Jiao, J. Michalicka, G. S. Was

Department of Nuclear Engineering and Radiological Sciences, University of Michigan

Self-ion irradiations are capable of producing samples at high fluences over a short time frame. However, microstructure and microchemistry by heavy ion irradiations need to be validated against those from neutron irradiations. Microstructure/radiation-induced segregation (RIS) of 304L SS irradiated in BOR60 to 46 dpa at 320°C was used as the reference irradiation condition. Four self-ion irradiations (46 dpa at 500°C; 30 dpa at 600°C and 46 and 260 dpa at 380°C) were chosen for comparison to the neutron irradiations. Self-ion irradiation to 260 dpa at 380°C produced similar dislocation loop size, and density and precipitate size as neutron irradiation to 46 dpa at 320°C. Self-ion irradiation to 30 dpa at 600°C produced the highest level of segregation at the grain boundary. The results suggest that the best way to emulate neutron irradiated microstructure in stainless steels using self-ion irradiation may be to study microstructure evolution and RIS separately. The microstructure of the recently completed 46 dpa at 380°C irradiation is being examined. Preliminary atom probe tomography (APT) result reveals radiation-induced Ni/Si-rich precipitates and segregation of Si and P at the grain boundary.

Support for this research was provided by the U.S. National Nuclear Security Administration (NNSA) under award # 91752



Segregation of Si and P at the grain boundary in 304L SS following  $\text{Fe}^{++}$  irradiation to 46 dpa at 380°C as revealed by APT. The dimensions of the box are 55nm x 55nm x 75nm.

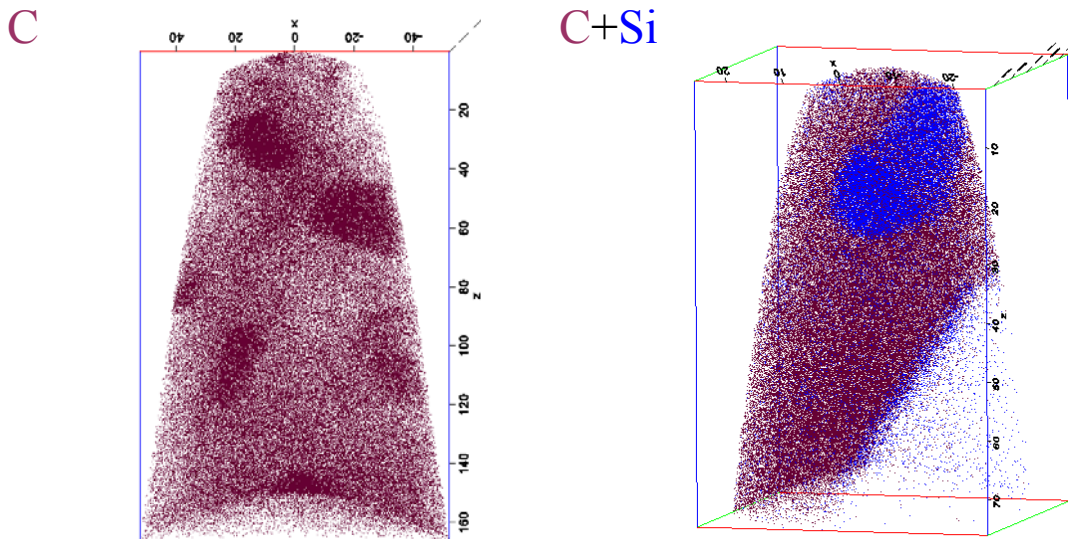
# PHASE STABILITY IN HEAVY ION IRRADIATED FERRITIC-MARTENSITIC ALLOYS AT HIGH FLUENCES

G. S. Was, Z. Jiao, J. Wharry, G. Yu, E. Beckett

Department of Nuclear Engineering and Radiological Sciences, University of Michigan

Understanding microstructure development in materials irradiated to high dose is, in a sense, the holy grail of materials performance in reactor systems. Fast reactor ducts will likely see damage levels of 200 dpa, and for the Traveling Wave Reactor to be come a reality, the clad and some structural materials must withstand 500-600 dpa. Water-based test reactors (ATR, HFIR) can provide ~3-5 dpa/yr level. Fast reactors accumulate damage more quickly but are limited to ~20 dpa/yr. As such, only ion irradiation is capable of providing the required levels of damage in reasonable time frames. Ferritic-martensitic alloys (T91, HCM12A and HT-9) were irradiated up to 500 dpa at temperatures 400-500°C at MIBL. Radiation-induced precipitates were investigated using atom probe tomography (APT). Typically, four types of precipitates were observed in heavy-ion irradiated F-M alloys. They are Ni/Si-rich, Cu-rich and Cr-rich precipitates and Cr-rich carbides. Irradiation to 500 dpa at 500°C resulted in high volume of Cr-rich carbides as seen in the figure bellow.

Support for this research was provided by the U.S. DOE under contract DE-FG07-07ID14894, and DE-AC07-05ID14517, and TerraPower.



APT C atom maps of HCM12A (left) and C+Si atom maps of HT-9 (right) following 5 MeV Fe<sup>++</sup> irradiation to 500 dpa at 500°C. Cr-rich carbides are seen in both images. One large Ni/Si-rich precipitate (blue cluster) is also seen in the right image.

# ION IRRADIATION-INDUCED DEGRADATION OF REACTOR STRUCTURAL MATERIALS

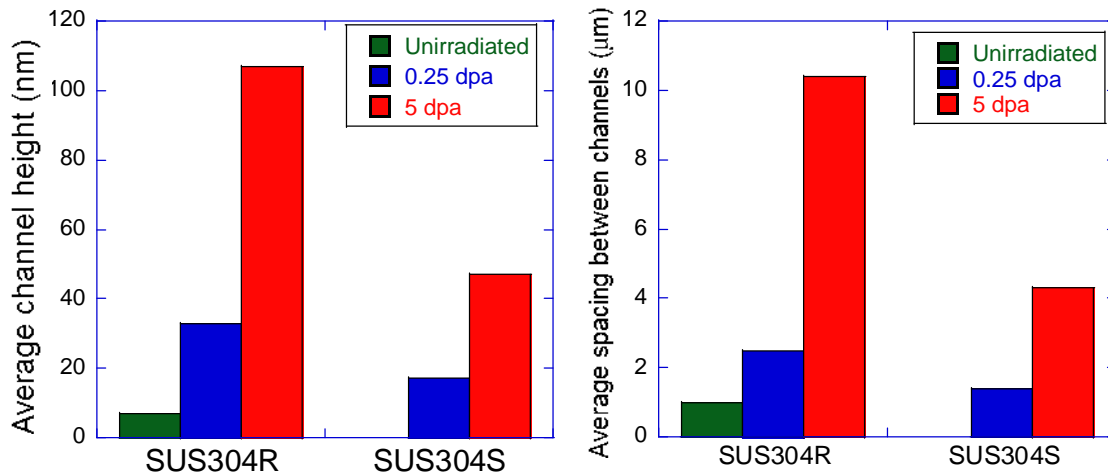
Z. Jiao<sup>1</sup>, G. S. Was<sup>1</sup>, T. Miura<sup>2</sup>, K. Fukuya<sup>2</sup>

<sup>1</sup>Department of Nuclear Engineering and Radiological Sciences, University of Michigan

<sup>2</sup>Institute of Nuclear Safety System, Japan

The Institute for Nuclear Safety Systems (INSS) and the University of Michigan have recently concluded a joint, three-year program on ion irradiation-induced degradation of reactor structural materials, aimed at exploring the processes and mechanisms that contribute to materials degradation in light water reactors arising from irradiation, such as irradiation assisted stress corrosion cracking, embrittlement, deformation modes and mechanisms. The objective of the program is to develop an understanding of these irradiation-induced degradation processes using ion irradiation as an emulation for neutron irradiation. The program is experimentally based, and focuses on irradiation with light ions (e.g., 2-3 MeV protons) and heavy ions (e.g., 5 MeV Ni and Fe ions). Important conclusions include: 1). Both average step height and spacing in proton irradiated samples are significantly larger than those in Fe<sup>++</sup> irradiated samples, probably due to the large difference in irradiation depth. 2). Step height and spacing increased with irradiation depth and saturates when at least 1/3 of grain size is irradiated. 3). Irradiation dose at the damage peak is not the main factor determining step height and spacing because the peak is very narrow and may not be sufficient to block glide dislocations. 4). SUS304S, with a small grain size of ~11  $\mu\text{m}$  shows a smaller step height and spacing compared to SUS304 with a grain size of ~30  $\mu\text{m}$ .

Support for this research was provided by The Institute for Nuclear Safety Systems, Japan.



Grain size effect on average dislocation channel height and spacing in proton irradiated SUS304. Irradiations were conducted at 300°C. Samples were stained in argon to 2% at 300°C. SUS304R: regular grain size of 30 $\mu\text{m}$ . SUS304S: small grain size of ~11 $\mu\text{m}$ .

# ATOMIC LAYER DEPOSITION OF NICKEL NITRIDE THIN FILMS FROM A VOLATILE AND THERMALLY STABLE NICKEL DIAZADIENATE PRECURSOR

T. J. Knisley<sup>1</sup>, M. J. Saly<sup>2</sup>, R. Kanjolia<sup>2</sup>, C. H. Winter\*<sup>1</sup>

<sup>1</sup>Department of Chemistry, Wayne State University

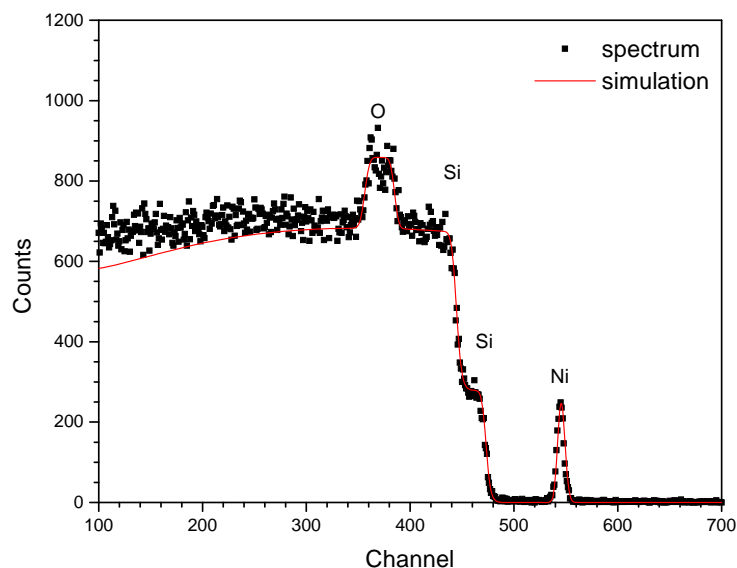
<sup>2</sup>SAFC Hitech, Haverhill, MA

Nickel nitride ( $\text{Ni}_x\text{N}$ ) films have been studied as an intermediate material for the formation of both nickel metal<sup>1</sup> and nickel silicide<sup>2a,b</sup> using chemical vapor deposition. Herein, we describe the ALD growth of nickel nitride thin films from bis(1,4-di-*tert*-butyl-1,3-diazabutadiene) nickel(II) ( $\text{Ni}(\text{tBu}_2\text{DAD})_2$ ) and 1,1-dimethylhydrazine. An ALD window for the deposition of nickel nitride films upon 500 nm thermal  $\text{SiO}_2$  was observed between 225 and 240 °C with a constant growth rate of 0.70 Å/cycle. X-ray photoelectron spectroscopy (XPS) showed all expected ionizations with carbon concentrations below the detection limit after argon ion sputtering. In lieu of preferential nitrogen sputtering in XPS, Rutherford backscattering spectrometry (RBS) and nuclear reaction analysis (NRA) were performed and subsequently revealed a varying Ni:N ratio of 2–4 for films deposited within the ALD window. AFM measurements revealed a RMS roughness value of 10.8 nm on an as-deposited film at 225°C. All as-deposited films were amorphous as determined by X-ray diffraction.

1. Li, Z.; Gordon, R. G.; Li, H.; Shenai, D. V.; Lavoie, C., *J. Electrochem. Soc.*, **2010**, 157, 679.

2. a) Li, Z.; Gordon, R. G.; Pallem, V.; Li, H.; Shenai, D. V., *Chem. Mater.*, **2010**, 22, 3060.

b) Lindahl, E.; Ottosson, M.; Carlsson, J.-O., *J. Vac. Sci Technol. A.*, **2010**, 28, 1203.



RBS spectrum and simulation using SIMNRA for one of the samples.

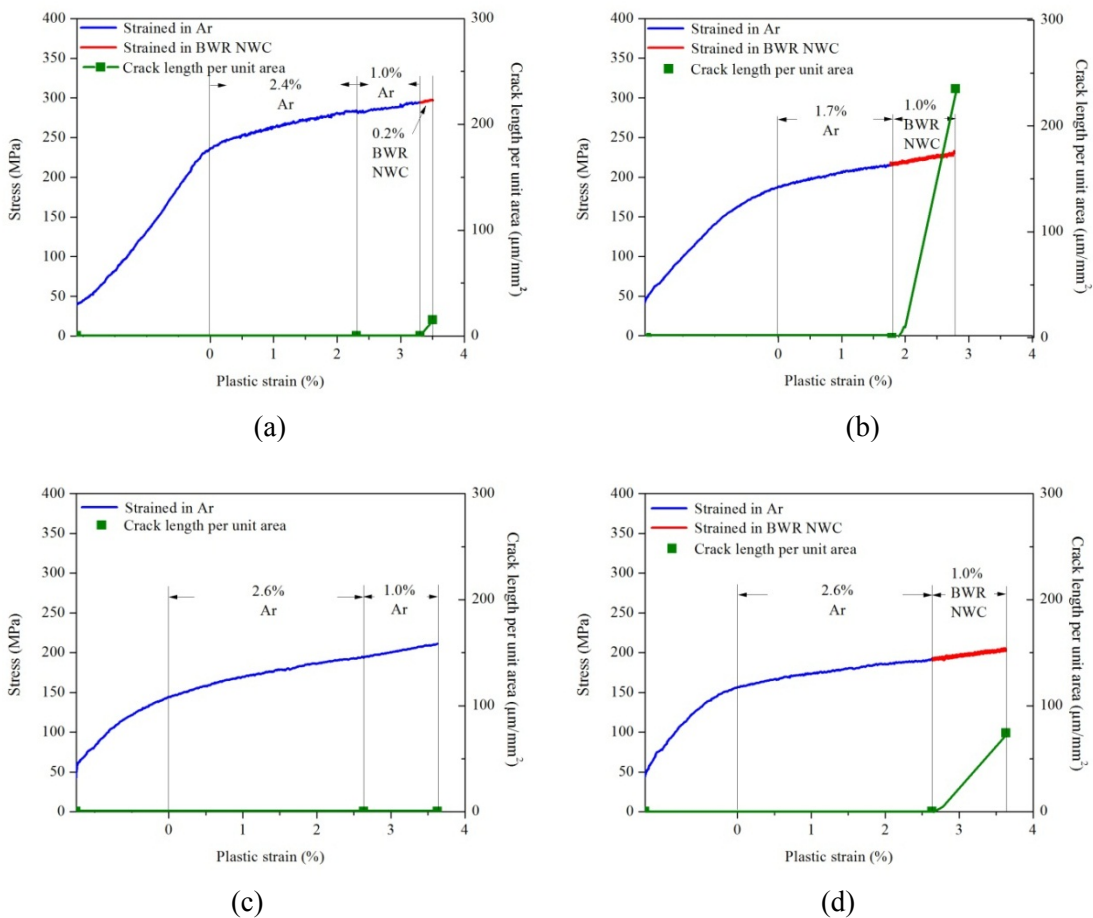
# EFFECT OF ENVIRONMENT AND PRESTRAIN ON IASCC OF AUSTENITIC STAINLESS STEELS

W. Lai, Z. Jiao, G. S. Was

Department of Nuclear Engineering and Radiological Sciences, University of Michigan

The effect of environment and prestrain on IASCC of austenitic stainless steels was investigated in post-irradiation CERT tests in Ar at 288°C and simulated BWR NWC. Two alloys susceptible to IASCC were selected for this study, which are commercial alloy 304 and high purity Fe-15Cr12Ni. Samples were irradiated to 5 dpa with 2 MeV protons at 360°C and strained to about 2% in Ar at 288°C. The results showed that the water environment is the key to inducing IASCC at 288°C. No intergranular cracking was observed in either alloy following straining in Ar up to ~3.5%. However, cracking occurred once the samples were subsequently strained to an additional 1% in simulated BWR NWC. Normal stress is critical in determining the crack initiation location in CP304 and Fe-15Cr12Ni when strained in simulated BWR NWC because the cracked grain boundaries were preferentially aligned perpendicular to the tensile direction.

Support for this research was provided by Electric Power Research Institute (EPRI) under contract EP-P35203/C15971.



Stress-strain curves and crack length per unit area versus strain for (a) CP304-1 and (b) CP304-2, (c) Fe-15Cr12Ni-1 and (d) Fe-15Cr12Ni-2 in different environments. All samples were irradiated to 5 dpa at 360°C with 2 MeV protons.

# IRRADIATION DAMAGE AND LOCALIZED DEFORMATION OF AUSTENITIC STAINLESS STEELS IN PWR ENVIRONMENT

M. Le Millier<sup>1</sup>, J. Crépin<sup>1</sup>, C. Duhamel<sup>1</sup>, F. Gaslain<sup>1</sup>, A. Pineau<sup>1</sup>, O. Calonne<sup>2</sup>, L. Fournier<sup>2</sup>, Y. Vidalenc<sup>2</sup>, E. Heripre<sup>3</sup>, O. Toader<sup>4</sup>

<sup>1</sup>Centre des Matériaux, CNRS UMR 7633, Mines ParisTech, France

<sup>2</sup>AREVA NP, France

<sup>3</sup>Laboratoire de Mécanique des Solides, CNRS UMR 7649, Polytechnique-X-Mines ParisTech, France

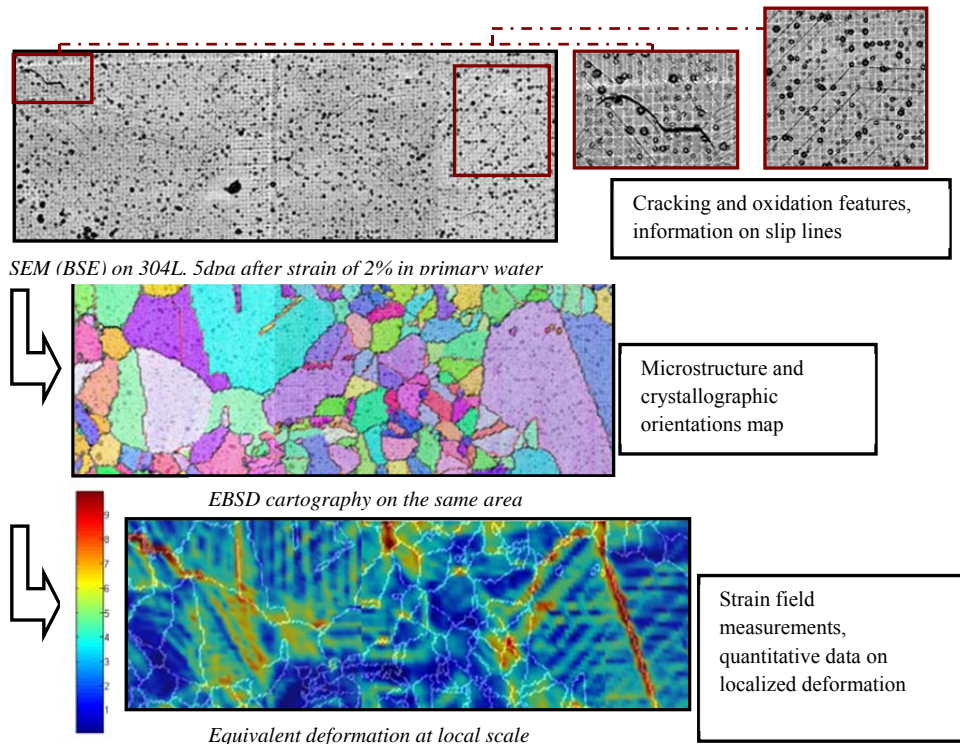
<sup>4</sup>Department of Nuclear Engineering and Radiological Sciences, University of Michigan

The purpose of this work is to determine initiation criteria for IASCC that take into account radiation dose, microstructural parameters of the alloy and quantitative mechanical data on the localized deformation.

To reach this goal, a protocol is developed to correlate crack initiation and propagation to crystallographic orientations and strain field measurements by using SEM digital imaging correlation technique coupled with EBSD cartography.

Thereby, 304L specimens were irradiated with 2 MeV protons at 360°C to 5 dpa and recently to 10 dpa. Those specimens are then strained to various macroscopic strains in PWR primary water. We observe intergranular cracks, which occurred on high angle boundaries, perpendicular to the tensile axis. The strain field analysis shows a strong heterogeneity, with localization near some grain boundaries.

This research is supported by the chair AREVA of Mines ParisTech graduate school



# ELIMINATING OXYGEN VACANCIES IN LITHIUM MANGANOSPINEL SYNTHESIZED BY HYDROTHERMAL METHODS

X. Hao<sup>1</sup>, B. M. Bartlett<sup>1</sup>, F. U. Naab<sup>2</sup>, O. Gourdon<sup>3</sup>

University of Michigan, Dept. of Chemistry

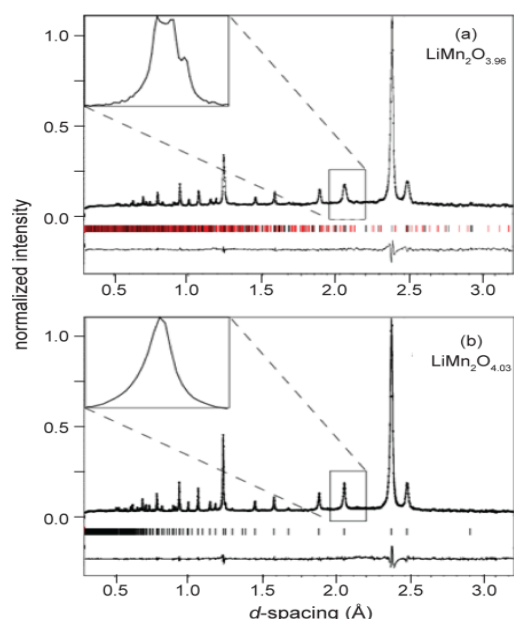
<sup>2</sup>Department of Nuclear Engineering and Radiological Sciences, University of Michigan

<sup>3</sup>Oak Ridge National Laboratory

In our research, lithium manganospinel ( $\text{Li}_{1+x}\text{Mn}_{2-x}\text{O}_{4-\delta}$ , lithium manganese oxide) has been synthesized by hydrothermal methods employing potassium permanganate, lithium hydroxide, and acetone as synthons. Materials prepared by this low-temperature route contain oxygen vacancies, which can be demonstrated by combining thermogravimetric analysis, differential scanning calorimetry, and cyclic voltammetry. Oxygen vacancies can be eliminated by a simple annealing treatment in 500°C air. Inductive coupled plasma-atomic emission spectroscopy and potentiometric titration was used to study the composition of the compounds. To determine the oxygen content directly in the materials, Rutherford backscattering analysis combined with nuclear reaction analysis has been applied to pressed pellets of our synthesized lithium manganospinel. However, the large intrinsic error and the small concentration of vacancies prevented us from making strong conclusions about oxygen vacancies.

To study this problem further, we performed neutron diffraction at Oak Ridge National Lab; the result matches our elemental analysis very well and provides structural detail on the oxygen vacancy sites within the lattice. At room temperature, Rietveld refinement of the powder neutron diffraction pattern shows an orthorhombic  $Fddd(\alpha 00)$  superlattice of the  $Fd\bar{3}m$  space group for hydrothermally synthesized lithium manganospinel. After annealing, oxygen vacancies are eliminated and the superlattice features disappear, illustrated in the Figure.

This work was supported by generous start-up funding from the University of Michigan. Neutron beam time at BL-11A at ORNL was sponsored by proposal IPTS-3920.



Neutron powder pattern obtained on POWGEN at 300 K on (a)  $\text{LiMn}_2\text{O}_{3.96}$  synthesized in air, and (b) the annealed  $\text{LiMn}_2\text{O}_{4.03}$  sample.

# STUDY OF MICROSTRUCTURE EVOLUTION UNDER PROTON IRRADIATION IN RECRYSTALLIZED ZIRCALOY-4

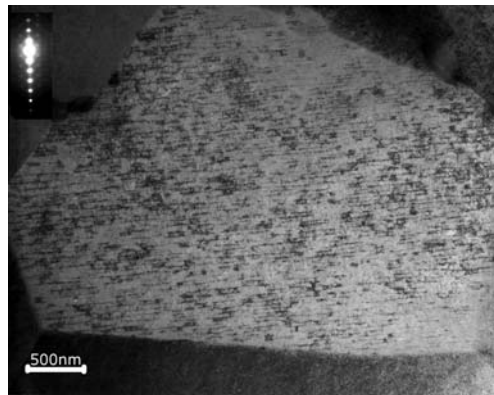
F. Onimus<sup>1</sup>, L. Tournadre<sup>1</sup>, J.-L. Béchade<sup>1</sup>, O. Toader<sup>2</sup>  
<sup>1</sup>CEA-Saclay, France

<sup>2</sup>Department of Nuclear Engineering and Radiological Sciences, University of Michigan

Zirconium alloys, used as cladding and structural material in the nuclear fuel assembly undergo deformation under irradiation. This deformation is due mainly to irradiation creep and growth. Contrary to creep which occurs under an external applied stress, growth occurs without any stress and has been clearly related by several authors to the crystal defects created under irradiation. It has been particularly shown that growth breakaway growth that occurs at high fluence (after 6 dpa) is related to the appearance of  $\langle c \rangle$  component dislocation loops. To improve our knowledge of the behavior of Zr alloys under irradiation, especially in PWR conditions, the CEA (Commissariat à l'Energie Atomique) has undertaken a research program using charged particle (protons and heavy ion) irradiations. The objective of this program is to provide insights into the evolution of the microstructure under irradiation up to high doses.

2 MeV proton irradiations were performed in March 2011 up to 12.5 dpa and in October 2011 up to 5 dpa and 19 dpa at 350°C on recrystallized zirconium alloy samples. Some of them have been pre-hydrided. The beam current measured on the sample holder was around 40  $\mu\text{A}$  leading to a damage creation rate (using 40 eV as displacement energy) of  $1.95 \times 10^{-5} \text{ dpa.s}^{-1}$ . After irradiation the rear side of the samples has been mechanically polished and Transmission Electron Microscopy (TEM) foils have been taken out of the samples. The irradiated side has been electro polished to approximately a 10  $\mu\text{m}$  depth under the surface and electro polishing was done on the rear side of the sample. The TEM observations were performed at CEA on two different TEMs: a Philips EM430 operating at 300 keV and a JEOL 2100 operating at 200 kV. The TEM observations have proved (see Figure) that after proton irradiation performed at 350°C,  $\langle c \rangle$  component dislocation loops are observed [1]. The loops have been observed at all irradiation doses studied. The effect of the hydrogen is currently being investigated. The results will be presented at TMS 2012 (oral presentation).

[1] Tournadre L., Onimus F. and al, *Experimental study of the nucleation and growth of c-component loops under charged particle irradiations of recrystallized Zircaloy-4*. To be published in JNM, TMS 2011 proceedings.



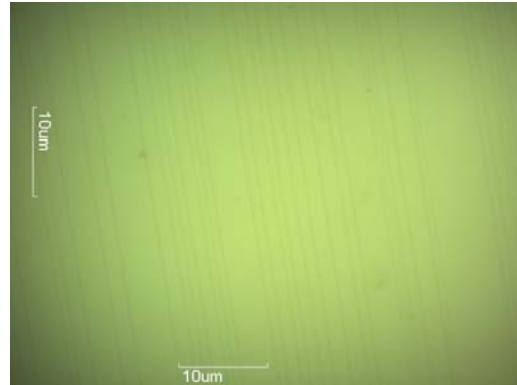
$\langle c \rangle$  component dislocation loops observed head-on using  $g=0002$  diffraction vector in recrystallized Zy-4 irradiated with 2 MeV protons at 350°C up to 12.5 dpa.

# ION IMPLANTATION OF BULK FERROELECTRIC MATERIALS ON POLYMER

R. M. Reano

Department of Electrical and Computer Engineering, Ohio State University

Ion implantation on a bulk ferroelectric material, using a small atomic mass ion, is conducted to produce a deeply buried damage layer. The majority of the ions are deposited in a relatively narrow spatial region of the sample where lattice defects are introduced by the transfer of energy to sample nuclei. The energy of the ions determines the depth of the damage layer. Our ion implantation run consisted of 195 keV  $\text{He}^+$  ions to a fluence of  $4 \times 10^{16}$  ions/cm<sup>2</sup>, and beam current of 0.25 mA/cm<sup>2</sup>. After implantation, the sample was found to be cracked along the left edge (Fig. at left). The crack may be due to the pressure produced by the mechanical clip holding it in the chamber. Optical inspection also revealed microcracks in the sample (Fig. at right). Methods to remove the microcracks are currently under investigation.



Optical micrograph of implanted ferroelectric material (left). The crack in the wafer may be due to the pressure produced by the mechanical clip holding it in the chamber. Optical micrograph on a 10 micrometer scale shows the presence of microcracks in the sample (right).

# EVOLUTION OF STRUCTURAL AND THERMOELECTRIC PROPERTIES OF INDIUM-ION-IMPLANTED EPITAXIAL GaAs

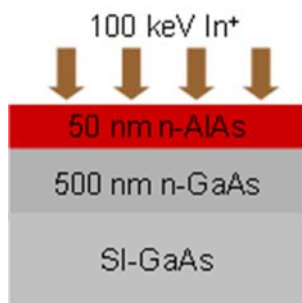
M.V. Warren<sup>1</sup>, A. W. Wood<sup>2</sup>, J. C. Canniff<sup>1</sup>, C. Uher<sup>2</sup>, R.S. Goldman<sup>1</sup>

<sup>1</sup>Department of Materials Science and Engineering, University of Michigan

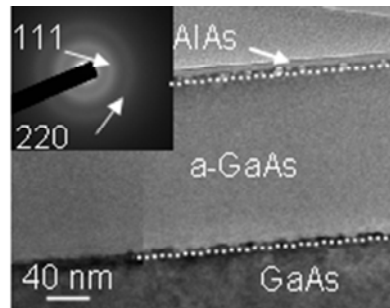
<sup>2</sup>Department of Physics, University of Michigan

Nanocomposite materials have been identified as promising candidates for high figure-of-merit thermoelectric materials. Of particular interest is the potential enhancement of the temperature-gradient-induced voltage (the Seebeck effect) using nanoscale inclusions for electron energy filtering. Recently, a new method for the fabrication of embedded metallic and semi-metallic particles has emerged, namely, “matrix-seeded growth,” which consists of ion-beam-amorphization, followed by nanoscale recrystallization via annealing. We have examined the structural and thermoelectric properties of GaAs:In nanocomposites prepared by matrix-seeded growth. We use a 50 nm AlAs sputter-mask to increase the retained concentration of In<sup>+</sup> ions in GaAs as a path towards the formation of nanoscale InAs crystals in an amorphous GaAs matrix. We studied the effects of three doses:  $3.8 \times 10^{15}$  (“low”),  $3.8 \times 10^{16}$  (“medium”) and  $3.8 \times 10^{17}$  cm<sup>-2</sup> (“high”). The low and medium fluence films consist of a residual AlAs layer on a-GaAs, whereas the high fluence film consists of an a-GaAs layer with crystalline remnants. Following RTA, the low and medium fluence films consist of a recrystallized GaAs layer with stacking faults likely due to simultaneous recrystallization from the AlAs and crystalline GaAs interfaces, while the high fluence film is polycrystalline. The Seebeck coefficient ( $S$ ) increases with ion fluence, with the high fluence film showing both electrons ( $T < 10$  K) and holes ( $T > 10$  K) as charge carriers with corresponding phonon drag peaks of -12 mV/K at 4 K and +2 mV/K at 15 K. This sign conversion of  $S$  indicates an  $n$ -to- $p$ -type conversion, presumably due to the migration of Si dopant atoms from Ga to As sites. These results suggest a new path for the formation of embedded semiconductor nanocomposites for thermoelectrics. Work is underway to identify the annealing conditions required to achieve embedded InAs nanocrystal formation in an amorphous GaAs-based matrix.

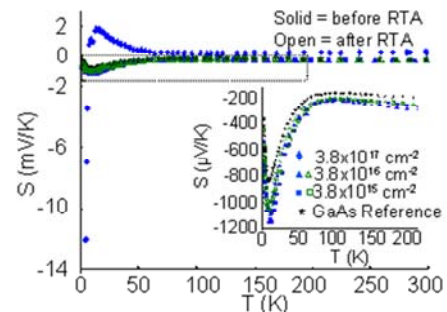
This work is supported in part by the GAANN Fellowship and the US Department of Energy, Office of Basic Energy Sciences as part of an Energy Frontier Research Center.



Cross-section of the implanted structure. In<sup>+</sup> is implanted through the AlAs sputter-mask into the GaAs film.



Cross-sectional transmission electron microscopy image of the medium dose film, with ~10nm AlAs and ~150 nm GaAs. The corresponding selected area diffraction, presented in the inset, reveals a predominately amorphous structure.



$S(T)$  for the low, medium, and high dose films, as well as a GaAs reference. As the implantation dose increases,  $|S|$  increases. For the highest dose, there is a transition from  $S < 0$  for  $T < 10$  K to  $S > 0$  for  $T > 10$  K, indicating a conversion from  $n$ -type to  $p$ -type conduction.

# RADIATION-INDUCED SEGREGATION IN FERRITIC-MARTENSITIC ALLOYS

J. P. Wharry, G. S. Was

Department of Nuclear Engineering and Radiological Sciences, University of Michigan

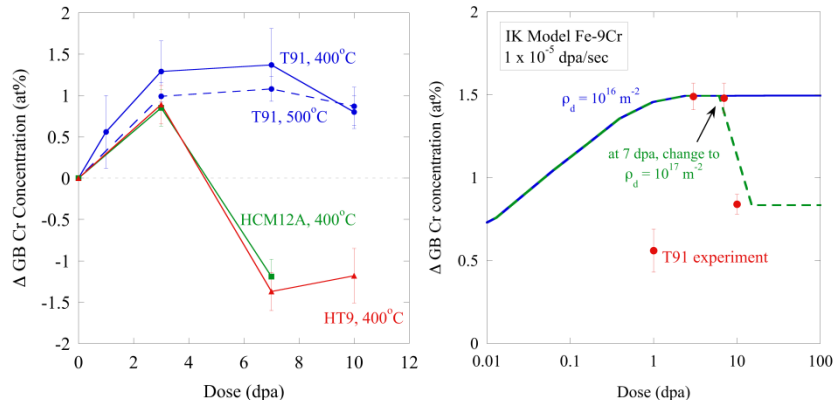
Radiation-induced segregation (RIS) is a non-equilibrium process by which alloying elements segregate at grain boundaries, under high temperature irradiation; it can have profound consequences on the mechanical properties and performance of the alloy. Ferritic-martensitic (F-M) alloys are structural material candidates for advanced fast reactors, so understanding the mechanism of RIS, particularly that of Cr RIS, in this class of steels is of great interest.

Three commercial F-M steels are studied: T91 (~9Cr), HT9 (~12Cr), and HCM12A (~11Cr). The alloys are irradiated with 2.0 MeV protons at a dose rate of  $10^{-5}$  dpa/sec at 400°C and 500°C to doses up to 10 dpa. RIS in all three alloys exhibits a complex dose dependence, in which low-dose ( $\leq 3$  dpa) Cr enrichment decreases in magnitude at higher doses (T91), or reverts to Cr depletion by 7 dpa (HT9, HCM12A). This behavior is shown in the left figure below. This complex dose dependence is attributed to the high and evolving sink density, which includes such features as a dislocation loops, laths, and various types of precipitates.

The inverse Kirkendall (IK) mechanism of RIS has been shown to be consistent with experimental measurements in austenitic stainless steels, and is hypothesized to also be consistent with RIS in F-M steels. For an Fe-9Cr steel subject to irradiation at  $10^{-5}$  dpa/sec at 400°C with fixed sink density of  $10^{16} \text{ m}^{-2}$  (approximately that measured in as-received T91), the IK mechanism predicts Cr RIS magnitudes on the same order as those measured by STEM/EDS in irradiated T91. However, the IK model predicts that RIS should saturate near 7 dpa, which is not consistent with experiments. But when a dose-dependent sink density is implemented into the IK model, RIS magnitude better follows dose dependence observed by STEM/EDS.

Future work involves refining the dose evolution within the IK model, as well as the dependence of RIS on temperature and bulk Cr concentration. A laboratory-purity Fe-9Cr F-M steel will also be irradiated and compared to T91 and IK model results.

This work is supported by the U.S. Department of Energy under grant DE-AC07-05ID14517.



Comparison of Cr RIS in proton-irradiated T91, HT9, and HCM12A as a function of dose (left), and comparison of T91 experimental Cr RIS measurements to Fe-9Cr Inverse Kirkendall model predictions (right).

# IN-SITU PROTON IRRADIATION CREEP AND MICROSTRUCTURE OF F-M STEEL T91

C. Xu, G. S. Was

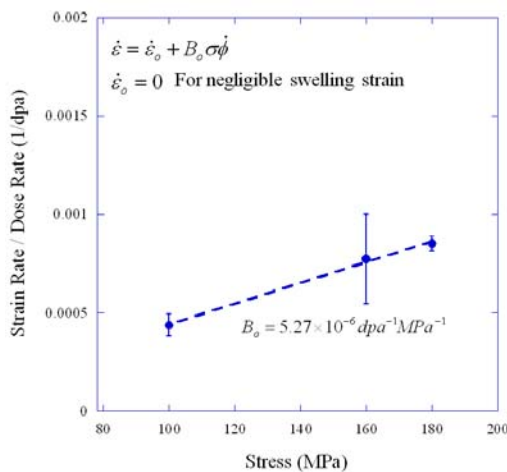
Department of Nuclear Engineering and Radiological Sciences, University of Michigan

In-situ irradiation experiments have been conducted to explore the stress and temperature dependence of irradiation creep in F-M alloy T91. Irradiation creep experiments were conducted at 500°C at three different stresses: 100MPa, 180MPa, and 160MPa. An additional creep experiment was conducted at 400°C and 160MPa to observe the effect of temperature. Preliminary analysis suggested a lack of temperature dependence and linear stress dependence for irradiation creep. Microstructure analysis with TEM and STEM showed significant amount of dislocation loops with a size distribution that is dependent on applied stress.

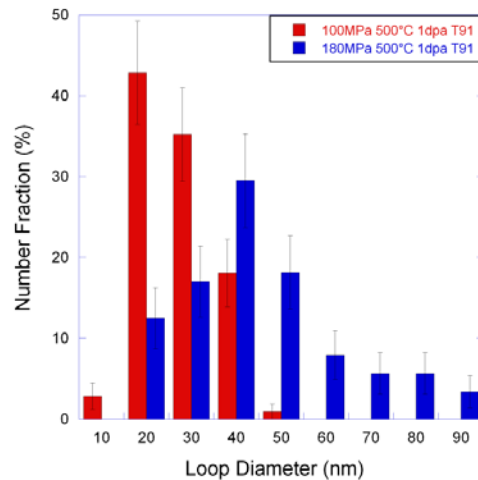
Irradiation creep rates were obtained by linear fits to in-situ strain measurements by laser speckle extensometer (LSE) and LVDT for each irradiated condition. Irradiation creep rates for 100MPa, 160MPa, 180MPa at 500°C are  $1.6 \pm 0.9 \times 10^{-9} \text{s}^{-1}$ ,  $2.33 \pm 1.8 \times 10^{-9} \text{s}^{-1}$ ,  $5.78 \pm 1.9 \times 10^{-9} \text{s}^{-1}$  respectively. By normalizing the creep rates to their respective dose rates, the creep compliance was obtained by measuring the slope of the data with respect to the applied stress. The data is plotted in the Figure (left), and the creep compliance was found to be  $5.24 \times 10^{-6} \text{dpa}^{-1} \text{MPa}^{-1}$ .

TEM analysis of the irradiation creep microstructure in the  $\langle 100 \rangle$  zone axis found large  $a_0 \langle 100 \rangle$  dislocation loops distributed homogenously within the material. Dislocation loops found within the 100MPa irradiation creep microstructure showed an average size of 20nm, while the 180MPa irradiation creep showed an average dislocation loop size of around 40nm, Figure (right). This observation is evidence that increasing applied stress increases the loop growth within T91 under irradiation at constant temperature.

Support for this research was provided by the Department of Energy under NEUP grant DE-AC07-05ID14517.



Irradiation creep rate normalized by dose rate plotted against applied stress.



Dislocation loop size distribution for irradiation creep of T91 at 500°C under 100MPa and 180MPa up to 1 dpa.

# MICROSTRUCTURE EVOLUTION IN FERRITIC-MARTENSITIC ALLOYS UNDER HEAVY ION IRRADIATED AT ELEVATED TEMPERATURE

G. Yu, J. P. Wharry, Z. Jiao, G. S. Was

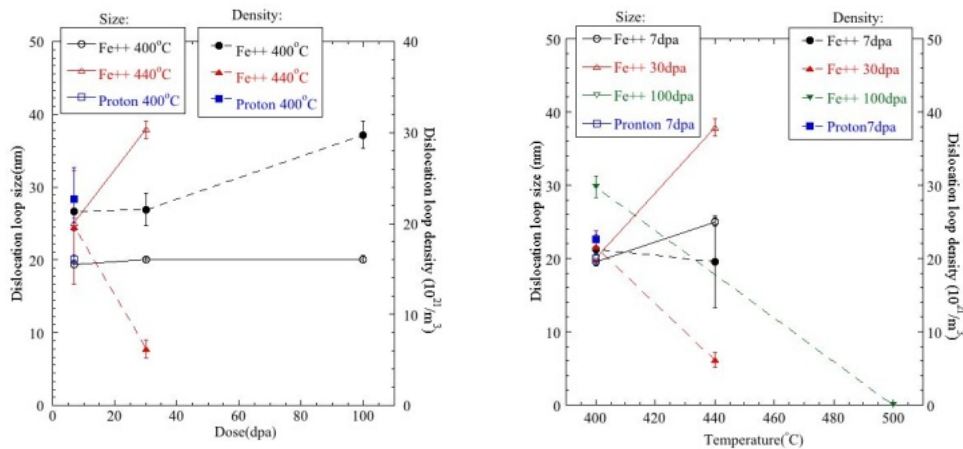
Department of Nuclear Engineering and Radiological Sciences, University of Michigan

At the doses and temperatures relevant to fast reactor operation, the microstructure of the T91 (9 wt.% Cr) and HCM12A (12 wt.% Cr) ferritic-martensitic alloys, as candidates for structural materials, evolves due to radiation-induced dislocation loop formation and growth, radiation-induced precipitation, destabilization of the existing precipitate structure, as well as the possibility for void formation and growth. These processes do not occur independently; rather, their evolution is highly interlinked. To extend the range of operation of structural materials in the sodium fast reactor, the irradiation-induced evolution of the microstructure at relevant temperatures and doses must be understood.

Both T91 and HCM12A alloys have been irradiated with 5.0 MeV Fe<sup>++</sup> ions (~1x10<sup>-3</sup> dpa/sec), accumulated to 7, 30 100 and 500 dpa at 400 and 500°C. TEM specimens were prepared by focused ion beam (FIB) milling. The irradiated microstructures were examined by TEM.

Irradiation induced defects, named defect clusters (black dots) or dislocation loops, voids and carbides were observed. The dislocation loop microstructure after Fe<sup>++</sup> irradiation is similar to that after proton irradiation. The loop size and density increase with dose and decrease with temperature. It seems that irradiation temperature plays a critical role in terms of dislocation loop microstructure (size and density) at high doses. There is no significant void formation as the size of voids is less than 5 nm and the density is less 3x10<sup>19</sup> m<sup>-3</sup>. The lath and subgrain structure is preserved under heavy ion irradiation. Carbides remain present on PAGBs, packet boundaries, and on some lath boundaries. The irradiation-induced Cr-rich, Cu-rich and Si/Ni-rich carbides precipitates were observed inside grain (on the matrix) of the HCM12A steels irradiated by Fe<sup>++</sup> ions accumulated to 500 dpa at 500°C.

Support for this research was provided by the U.S. DOE NEUP DE-AC07-05ID14517.



Dislocation loop size and density dose and temperature dependence.

# **IMPLANTATION EFFECTS ON THE ELECTRONIC PROPERTIES OF ZnO**

N. Feldberg<sup>1</sup>, S. M. Durbin<sup>1</sup>, C. N. Cionca<sup>2</sup>  
<sup>1</sup>Department of Physics, University at Buffalo  
<sup>2</sup>Department of Physics, University of Michigan

ZnO is an ultraviolet bandgap semiconductor of interest for a variety of optoelectronic applications and as a potential competitor to GaN. A major obstacle for junction devices based on this material is the difficulties faced in p-type doping.

This material exhibits surface bandbending on all crystalline faces, which is consistent with a branchpoint energy in the conduction band and believed to correlate strongly with the ability to p-type dope samples. However, experiments designed to experimentally measure the branchpoint energy point to a value in the bandgap, in conflict with surface Kelvin probe microscopy and xray photoelectron spectroscopy.

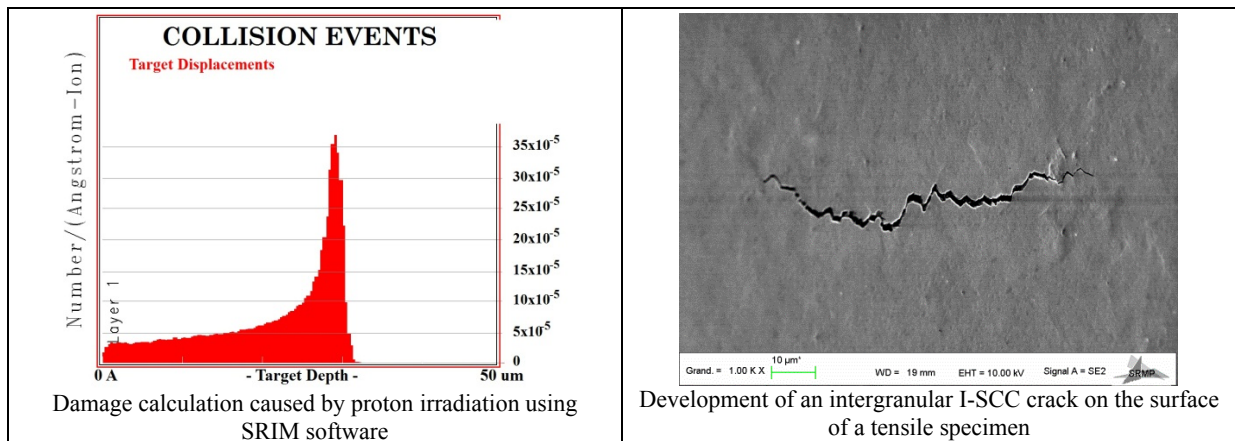
In order to improve our understanding of this material, we are investigating optical and electrical properties of ion-bombarded samples, which allow us to vary the bulk Fermi energy over a large range.

# STUDY OF IODINE-INDUCED STRESS CORROSION CRACKING OF ZIRCONIUM ALLOYS, INFLUENCE OF IRRADIATION AND STRESS BIAXIALITY

N. Mozzani<sup>1,2</sup>, E. Andrieu<sup>2</sup>, Q. Auzoux<sup>1</sup>, C. Blanc<sup>2</sup>, D. Le Boulch<sup>1</sup>  
<sup>1</sup>Commissariat à l'Energie Atomique; CEA Saclay, DMN/SEMI/LCMI,  
Gif-Sur-Yvette 91191, France  
<sup>2</sup>CIRIMAT/ENSIACET, Université de Toulouse, UPS/INPT/CNRS,  
4 allée Emile Monso, 31030 Toulouse Cedex 4, France

During incidental power transients in light water nuclear reactors, fuel cladding may fail due to the pellet-cladding interaction (PCI). The mechanism involved is iodine-induced stress corrosion cracking (I-SCC). I-SCC can be observed in laboratory and notably when testing cladding material in iodized methanol at room temperature. Neutron irradiation leads to a higher sensitivity to I-SCC and several studies showed the similarities between proton and neutron irradiation-induced microstructures.

In the current study, tensile specimens of fully recrystallized Zircaloy-4 are cut from thin sheets (0.5 mm thickness). The crack initiation domain of unirradiated Zircaloy-4 has been studied and boundaries are now known in terms of iodine concentration, strain rates and threshold plastic strain. Proton irradiations were carried out on a rectangular plate of the material. SRIM calculations showed that for a proton energy of 2 MeV, Bragg's peak is located at a depth of 30  $\mu\text{m}$ . The obtained irradiation dose was 2 dpa at 60% of the peak's depth. The irradiation temperature was 350°C. Testing in iodized methanol specimens cut from this plate should bring insights to the effect of irradiation on the initiation of intergranular I-SCC cracks. Stress biaxiality ratio effect on crack initiation will be investigated using notched specimens.



# BISMUTH INCORPORATION IN GaAsBi FILMS GROWN BY MOLECULAR BEAM EPITAXY

G. Vardar<sup>1</sup>, M. V. Warren<sup>1</sup>, M. Kang<sup>1</sup>, S. Jeon<sup>1</sup>, R. S. Goldman<sup>1,2</sup>

<sup>1</sup>Department of Materials Science and Engineering, University of Michigan

<sup>2</sup>Department of Physics, University of Michigan,

Due to the significant bandgap reduction associated with Bi incorporation, GaAsBi alloys have been proposed for high-efficiency solar cells and high performance infrared detectors. To date, the relationship between Bi incorporation mechanisms and the electronic and optical properties of GaAsBi alloys is not well understood. For example, the synthesis of GaBi has not been reported; therefore, the GaBi crystal structure and lattice parameters based upon density functional theory are typically used to interpret x-ray diffraction data. Here, we are investigating the growth, structure, and optoelectronic properties of GaAsBi alloy films. We grow GaAsBi alloy films by molecular beam epitaxy (MBE) and examine their optical and electrical properties with photoluminescence and electron transport measurements. To estimate the bismuth content in the films, we use a combination of high-resolution x-ray diffraction (HRXRD) and Rutherford backscattering spectroscopy (RBS). The HRXRD data allows us to determine the strain of the GaAsBi layer with respect to the GaAs substrate. The strain is then used to calculate the Bi content of the GaAsBi layer assuming that the lattice constant of GaAsBi varies linearly with increasing Bi content [1]. For comparison, we use RBS to determine the bismuth content of the GaAsBi films. The backscattered spectra for channel-to-energy conversions are simulated with SIMNRA [2] and the bismuth content and film thickness are adjusted to match the RBS data. For thick (~100nm) films, the agreement between HRXRD and RBS determination of Bi concentration is within 15%. However, for thin (~30nm) films, there is a large discrepancy between the HRXRD and RBS determination of the Bi concentration. Together, these results suggest a significant film thickness dependence of Bi incorporation into GaAsBi films.

We gratefully acknowledge the support of the National Science Foundation through Grant DMR-1006835. G. V. acknowledges the support of the Fulbright Foreign Student Fellowship.

[1] S. Tixier, M. Adamcyk, T. Tiedje, S. Francoeur, A. Mascarenhas, P. Wei, F. Schiettekatte, *Appl. Phys. Lett.* 82, 2245 (2003).

[2] M. Mayer, SIMNRA User's Guide 6.05, Max-Planck-Institut für Plasmaphysik, Garching, Germany, 2009

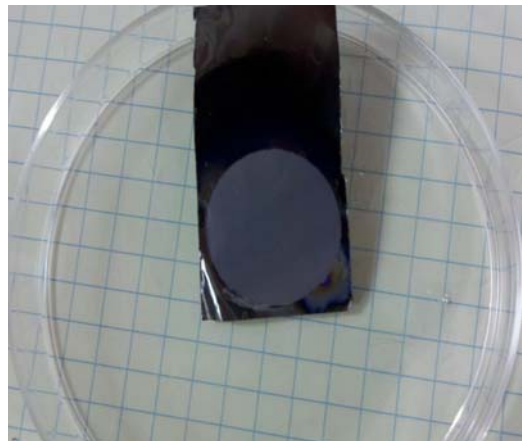
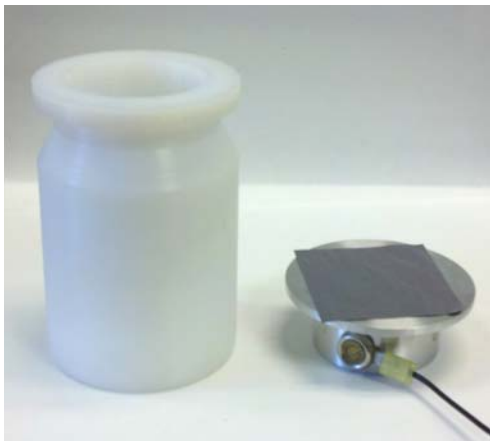
## DEVELOPMENT OF ONE-SIDED OXYGEN TARGETS FOR EXOTIC BEAM STUDIES

M. Febraro<sup>1</sup>, F.D. Becchetti<sup>1</sup>, M. Ojaruega<sup>1</sup>, R.O. Torres-Isea<sup>1</sup>, J.J. Kolata<sup>2</sup>, A. Roberts<sup>2</sup>

<sup>1</sup>Department of Physics, University of Michigan

<sup>2</sup>Department of Physics, University of Notre Dame

The objective of this project was to develop one-sided oxygen targets for use in exotic radioactive nuclear beam (RNB) studies. A technique for the preparation of large reasonably uniform one-sided targets using electrochemical oxidation of thin tantalum foils in water has been developed. Targets with an active area of 25 mm diameter (and larger) have been prepared using a constant-current source in 0.1% KI solution in deionized H<sub>2</sub>O. KI was used as an electrolyte to increase solution conductivity. The areal density of oxygen in the targets was measured using Rutherford backscatter analysis (RBS) at the Michigan Ion Beam Laboratory (MIBL). In addition to the anodization process, a method for chemical etching tantalum foils to a desired thickness using a mixture of nitric, sulfuric, and hydrofluoric acids has been developed. Currently, additional experiments at the MIBL are in the planning stages using the  $^{16}\text{O}(^3\text{He},n)^{18}\text{F}$  reaction to obtain the areal density of oxygen from the decay of  $^{18}\text{F}$ . These results will be compared to the previous RBS analysis. Testing of the targets will be conducted at the UM-UND *TwinSol* RNB facility as a joint project between the University of Michigan and the University of Notre Dame funded by grants from the National Science Foundation (NSF, PHY063981).



High density polyethylene (HDPE) anodization cell with tantalum foil located on top the anode plate (left). A prepared Ta<sub>2</sub>O<sub>5</sub> oxygen target on tantalum foil after chemical etching and anodization (right).

# EXPERIMENTAL STUDY OF IASCC OF STAINLESS STEELS IN RELATION TO IRRADIATION INDUCED PLASTICITY MECHANISMS

B. Tanguy<sup>1</sup>, S. Cissé<sup>1</sup>, C. Guerre<sup>1</sup>, O. Toader<sup>2</sup>

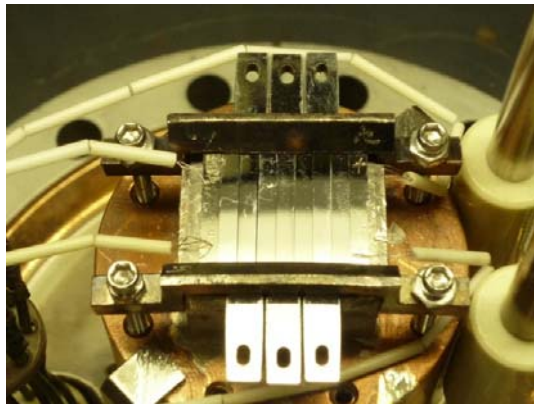
<sup>1</sup>CEA-Saclay, France

<sup>2</sup>Department of Nuclear Engineering and Radiological Sciences, University of Michigan

Component degradation by irradiation is a primary concern in both current reactor systems as well as advanced designs and concepts where the demand for higher efficiency and performance will be considerably greater. Among degradation mechanisms, IASCC (Irradiation Assisted Stress Corrosion Cracking) is of great importance as it has been evidenced that it may affect austenitic stainless steels (SS) used for internal structures of both BWR (boiling water reactor) and PWR (pressurized water reactor). IASCC is a complex degradation mechanism involving several contributors, making it far from being fully understood. Some of the material modifications due to irradiation (RIS, irradiation hardening) appear early in life, whereas others (swelling) appear at high levels of irradiation. Within the frame of PWR life extension, swelling is expected to occur at high dose levels so that the development of swelling in SS in PWR conditions (dose rate of  $\sim 5$  to  $10 \times 10^{-8}$  dpa/s and temperature of  $\sim 340^\circ\text{C}$ ) is still a subject of research activity and role of swelling on plasticity and then on the IASCC is an open question.

Within the frame of a better understanding of IASCC mechanisms, the CEA (Commissariat à l'Energie Atomique) has initiated studies to understand the interaction between plasticity mechanisms (especially microplasticity localization) and stress corrosion cracking (SCC) of irradiated austenitic SS. This study will focus on three main points: (i) the modification of plasticity mechanisms, particularly localization of plastic deformation due to irradiation with protons, (ii) the modification of plasticity localization due to the presence of cavities or bubbles (induced by He), and iii) the effect of these plasticity mechanisms modifications on the SCC susceptibility of irradiated material.

This year, 3.2 MeV protons irradiations were performed in October 2011 on two batches of tensile specimens up to 0.5 and 3 dpa at  $350^\circ\text{C}$  on SA 304 stainless steel in order to prepare specimens dedicated to the first point of this study. SCC tests in autoclaves are planned for the beginning of 2012 with PWR primary water environment (1200ppm B, 2ppm Li, 30 cc/kg  $\text{H}_2$ ,  $340^\circ\text{C}$ , 155 bars). Tensile load will be applied to the specimens with damage induced by hydrogen. After testing, IASCC sensitivity will be characterized by fracture surface, and TEM.



Sample holder (designed by MIBL) in order to irradiate tensile specimens using 3.2 MeV protons.

# **SYNTHESIS OF SiC HARVESTER PARTICLES FOR HIGH EFFICIENCY PHOTOVOLTAICS**

A. Rockett, S. Martin, K. Nygren  
Department of Materials Science and Engineering  
University of Illinois at Urbana Champagne

Photovoltaic conversion of solar energy directly to electricity represents one of the most promising methods for supplying global energy needs in the coming years. However, the current technologies are limited in their ability to capture this energy with high efficiency. One opportunity to improve this efficiency is to introduce “harvester” particles in a semiconductor matrix from which a photovoltaic device is produced that can absorb high energy photons and produce a larger amount of electric current in the output of the device than would normally be possible. The Rockett Group, including undergraduate student Sam Martin and former visiting scholar Kelly Henderson, aims to achieve this higher current output by introducing silicon carbide (SiC) precipitates in a silicon (Si) matrix. These particles in the planned work will absorb high energy light and will release high energy electrons into a surrounding Si matrix under conditions that will promote the generation of two free electrons rather than the one normally generated. The research is being initiated by implantation of carbon atoms into the Si matrix and subsequent annealing of the implanted Si to produce a fine distribution of SiC particles in the Si matrix at a controlled location. The work performed at MIBL is the implantation step. Subsequent annealing is being carried out in the Rockett laboratories and samples are being tested to demonstrate carrier multiplication at the University of Oregon at Eugene, which is the lead institution in this collaboration. Success has the potential to significantly increase device efficiency without undue additional expense. This holds the potential to significantly reduce the cost per kilowatt hour of the final electricity, which is key to achieving competitive pricing in energy generation compared to existing technologies.

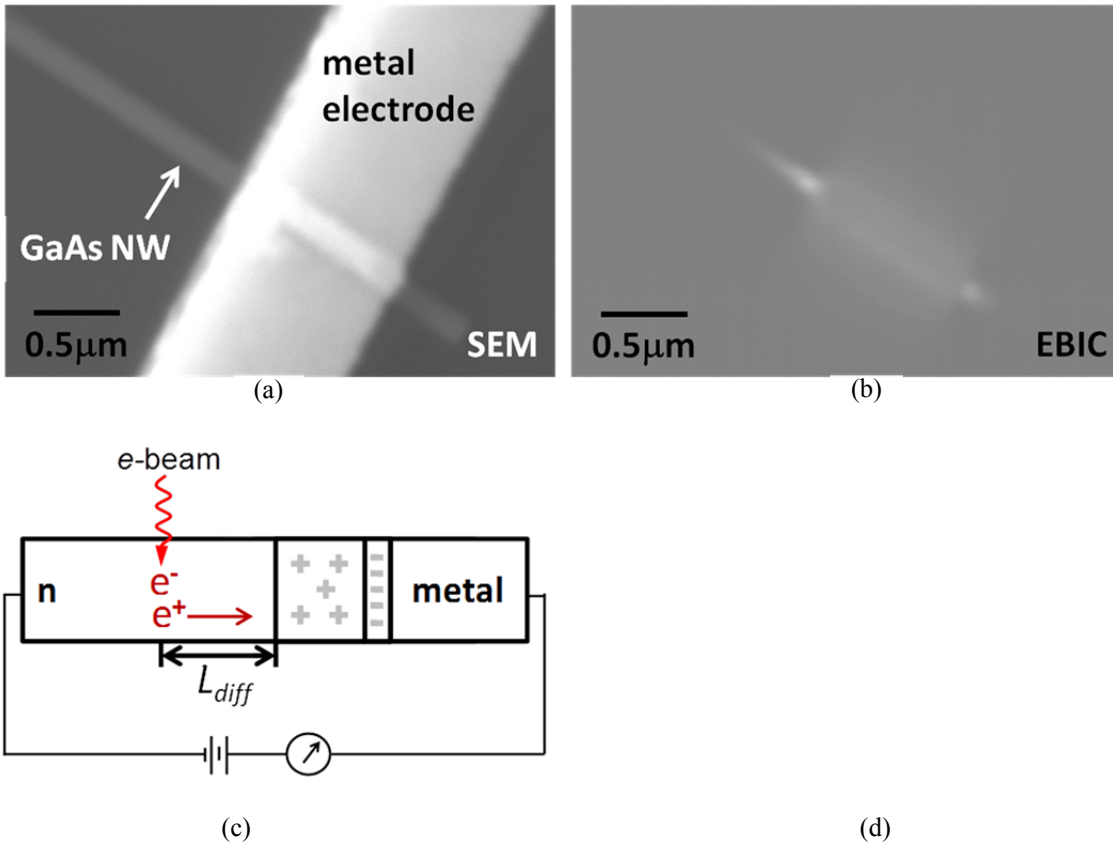
# STUDYING CARRIER DYNAMICS IN GaAs NANOWIRES

S. B. Cronin

Department of Electrical Engineering, University of Southern California

In this study, we grow GaAs nanowires by metal organic chemical vapor deposition (MOCVD).  $pn$  junctions and Schottky junctions are created in the nanowires using ion implantation at the Michigan Ion Beam Laboratory at the University of Michigan. Using an electron beam induced current (EBIC) technique, we measure the spatially mapped electron beam-induced current to reveal various characteristics about the carrier dynamics, such as minority carrier diffusion lengths. The figure below shows a schematic diagram of the experimental setup for this measurement. A fundamental understanding of these characteristics will be important for utilizing these nanowires for solar energy conversion. By applying a bias voltage to the same devices, we measure the photoconductivity spectra in the 450nm - 2000nm wavelength range. In addition to the spectral information, we will measure the quantum efficiency of these devices as a function of doping concentration, element, acceleration voltage, and post-annealing processing.

This work is supported as part of the Center for Energy Nanoscience, an Energy Frontier Research Center funded by the U.S. Department of Energy, Office of Science, Office of Basic Energy Sciences under Award Number DE-SC0001013.



SEM image of a  $\text{Al}_x\text{Ga}_{1-x}\text{As}$ -passivated GaAs nanowire device (a) and corresponding EBIC image (b). Conceptual diagram illustrating the formation of electron beam induced current (c) and EBIC profiles along wire axis for passivated and bare nanowires (d).

# **THE EFFECT OF HIGH-FLUORIDE TREATMENTS ON SURFACE CHARACTERISTICS OF DENTAL RESTORATIVE MATERIALS**

B. González-Cabezas, B. Kim, S. Flannagan  
University of Michigan School of Dentistry

Various restorative materials are widely used in the operative treatment of dental caries lesions. Concomitantly, treatment plans will often include the use of fluoride-based products designed to strengthen tooth enamel. However, the effect of high fluoride concentrations on the physical integrity of the restorative products is not fully understood.

This investigation aims to evaluate the effect of high-concentration fluoride products (gels, varnishes and rinses) on the surface characteristics of light-cured resin-based composites and glass ionomer restorative materials. Surface hardness, as well as surface roughness (using the Dektak 3 Surface Profile Measuring System at the Michigan Ion Beam Laboratory) will be among the parameters measured. This project is in the early stages therefore no significant results are available at this time.

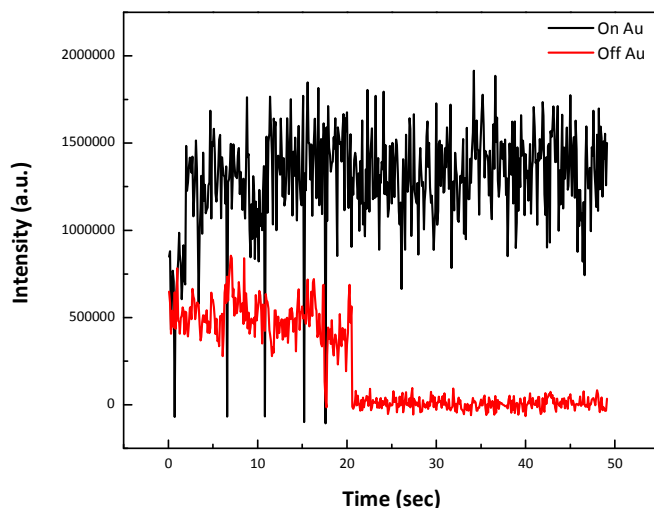
Funding is through UM School of Dentistry internal sources.

# PLASMON-ENHANCED SINGLE-MOLECULE FLUORESCENCE FOR SUPER-RESOLUTION IMAGING

Jessica E. Donehue, Julie S. Biteen  
Department of Chemistry, University of Michigan

In this work, gold nanorod and gold nanoisland substrates were developed and utilized in plasmon-enhanced fluorescence for single-molecule super-resolution imaging of small dye molecules and fluorescent proteins. Plasmon modes are the collective oscillations of free electrons in small metal particles that give rise to locally enhanced fields. These locally enhanced fields greatly affect the photophysical properties of nearby fluorophores. Plasmon coupling holds much promise for increasing fluorescence, and fluorophores coupled to plasmon modes are known to demonstrate enhanced absorption, faster radiative rates, increased quantum yields, and decreased photobleaching. In this project, we apply this near-field interaction to isolated single-molecule emitters (both organic dyes and fluorescent proteins) and observe both amplified fluorescence and increased photostability. The localization accuracy of single-molecule fluorescence is mainly limited by the number of emitted photons collected. Therefore, by amplifying the emission of a fluorophore, we can determine its position with nanometer-scale accuracy and acquire super-resolution images.

In the Michigan Ion Beam Laboratory, the Dektak3 profilometer was used to collect precise measurements of ultra-thin PMMA films spun onto the surface of our gold substrates. As fluorescence of a single-molecule emitter can be quenched by placing it directly on a metal surface, the PMMA served as a spacer layer to prevent quenching. However, because plasmon coupling is a near-field interaction, it was important to measure the film thickness to ensure the films were not too thick, as this would diminish the enhancement seen from coupling.



Time trace of single-molecule Cy3 (a fluorescent organic dye) both on and off gold nanorods. The emission intensity and “on-time” are both increased in Cy3 by coupling it to gold.

# MITIGATION STRATEGY FOR IASCC IN AUSTENITIC STAINLESS STEELS

Z. Jiao<sup>1</sup>, G. Was<sup>1</sup>, P. Chou<sup>2</sup>

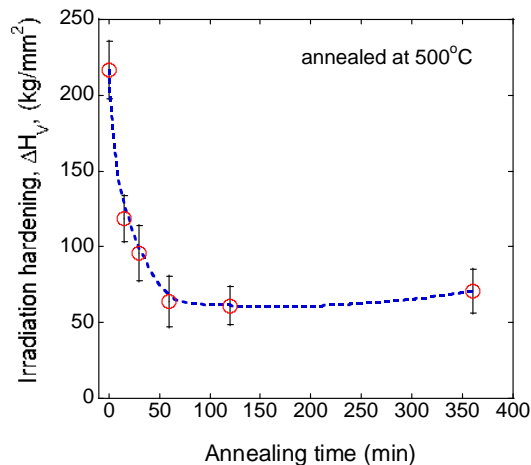
<sup>1</sup>Department of Nuclear Engineering and Radiological Sciences, University of Michigan

<sup>2</sup>Electric Power Research Institute

Irradiation assisted stress corrosion cracking (IASCC) is the primary form of core component cracking in light water reactors. The ultimate goal of this project is not only to understand the mechanism of IASCC, but to provide a mitigation strategy for components under service and a guide for alloy design for future reactors. Post-irradiation annealing (PIA) has been demonstrated as a potential mitigation method for IASCC in stainless steels. However, the reason that PIA may lead to the mitigation of IASCC is not well understood. This project is intended to understand the mitigation mechanism of PIA through its relationship with localized deformation in proton-irradiated austenitic stainless steels.

A commercial grade 304SS that is very susceptible to IASCC in simulated BWR environment was selected for this study. Samples were irradiated to 10 dpa using 2 MeV protons at 360°C at Michigan Ion Beam Laboratory (MIBL). PIA of irradiated samples annealed at 500°C for different lengths of time was conducted in a vacuum furnace. Microhardness was characterized using a microhardness indenter after each annealing treatment. The figure shows the mitigation of irradiation hardening as a function of annealing time. Irradiation hardening relates to the irradiation microstructure. Therefore, a decrease in irradiation hardening indicates the recovery of irradiation damage in the material.

Support for this research was provided by the Electric Power Research Institute (EPRI)



Remaining irradiation hardening as a function of annealing time at 500°C in CP304 following proton irradiation to 10 dpa at 360°C.

# TEACHING ACTIVITY

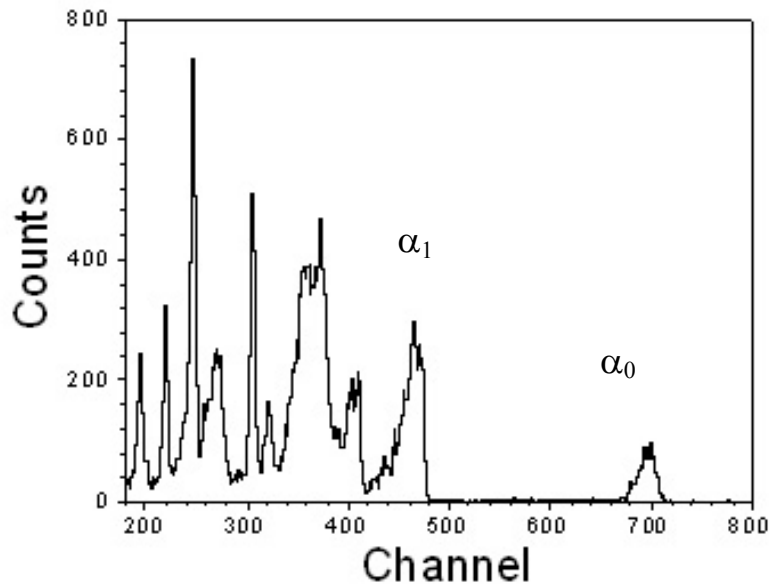
## NERS 425 LABORTORY ON NUCLEAR REACTION ANALYSIS

O. Toader, F. Naab, M. Atzmon

Department of Nuclear Engineering and Radiological Sciences, University of Michigan

For one laboratory in the NERS 425 course, students conducted an experiment to determine the stoichiometry of a  $Ti_xN_y$  sample using the reaction between a deuterium particle and a nitrogen nucleus:  $N^{14}(d,\alpha)C^{12}$ . Nuclear reaction analysis (NRA) is a well-established surface analysis technique. In this method, an energetic particle (deuterium – produced by the Tandem accelerator at MIBL) interacts with the nucleus of an N atom (from the target) to give a reaction product ( $\alpha$  particle) that can be measured. The students also use the backscattered yield from an RBS experiment to determine the amount of Ti in the sample by implementing simulation codes like RUMP or SIMNRA with the given experimental spectrum.

In the first class, and prior to the experiment, a short tutorial was given to the students on the accelerator, electronics, detectors, software, and vacuum components. After that, they worked independently in a few groups with just the basic support from the MIBL staff (required in the setup of the ion beam and the collection of the spectra). The students decided on a few parameters of the experiment (beam energy, time for spectrum acquisition, etc.) and after that each group obtains spectra similar to the ones in the figure.



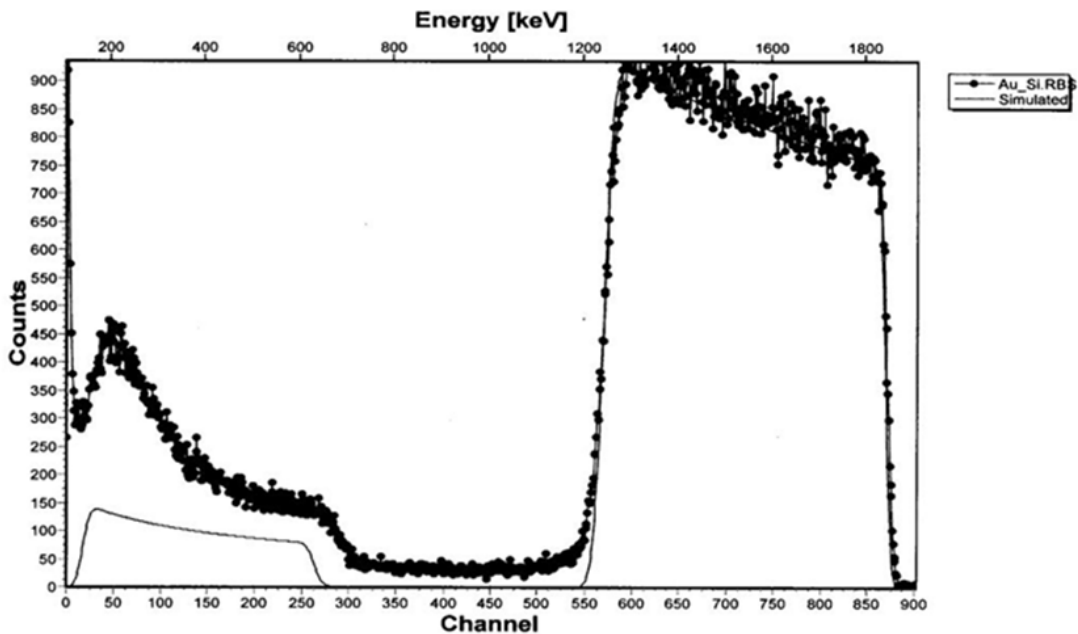
Typical NRA spectrum for the TiN film obtained during class.  
Conditions: beam energy: 1.4 MeV  $D^+$ , solid angle 5 msr., detector angle  $150^\circ$ .

# MSE 465 CLASS DEMONSTRATION AT MIBL

J. M. Millunchick

Department of Materials Science and Engineering, University of Michigan

MIBL hosted the MSE 465 class (Structural and Chemical Characterization of Materials) for an hour session to tour the facility and to demonstrate Rutherford Backscattering Spectrometry, a topic we covered in the class. A short tutorial was given on the accelerator, electronics, detectors, software, and vacuum components. As homework, the students were given a spectrum obtained at MIBL and asked to fit the data using SIMNRA, a simulation package commonly used in these experiments. The data for a gold film on a silicon substrate, along with the simulated spectrum, is plotted below.



RBS spectrum of Au film on a Si substrate. The spectrum was taken using a  $\text{He}^{++}$  ion beam at 2 MeV. The scattering angle was 160 degrees

# REFERENCES

## PUBLICATIONS AND PRESENTATIONS

Guo, Y., Li, H., Reddy, K., Shelar, H. S., Nittoor, V. R., and Fan, X., “Optofluidic Fabry-Pérot Cavity Biosensor with Integrated Flow-Through Micro-/Nanochannels,” *Appl. Phys. Lett.*, 98, 041104 (2011).

Tournadre L., Onimus F. and al., “Experimental study of the nucleation and growth of c-component loops under charged particle irradiations of recrystallized Zircaloy-4”. *J. Nucl. Mater.*, in press.

Youngsman, J., Gorman, G., Reimanis, I., Butt, D., *TRISO-coated Fuel Durability under Extreme Conditions*. TMS2011, San Diego, CA, February 2011.

M. Le Millier, O. Calonne, J. Crépin, C. Duhamel, F. Gaslain, E. Heripre, O. Toader, Y. Vidalenc, “Irradiation assisted stress corrosion cracking of stainless steels in a PWR environment (A combined approach)”, *Proceedings of the 15th International Conference on Environmental Degradation of Materials in Nuclear Power Systems* (2011).

M. Le Millier, O. Calonne, J. Crépin, C. Duhamel, F. Gaslain, E. Heripre, O. Toader, Y. Vidalenc, “Irradiation assisted stress corrosion cracking of stainless steels in a PWR environment (A combined approach)”, 15th International Conference on Environmental Degradation of Materials in Nuclear Power Systems, Colorado Springs, August 2011.

A.A. Campbell, G.S. Was, “Proton Irradiation-Induced Creep Effects in Pyrolytic Carbon and Graphite”, TMS Annual Meeting, San Diego, CA, February 27 – March 3, 2011.

Z. Jiao, V. Shankar, and G.S. Was, “Phase Stability in Proton and Heavy Ion Irradiated Ferritic-Martensitic Alloys” *J. Nucl. Mater.* 419 (2011) 52-62.

Z. Jiao, M. McMurtrey, G.S. Was, “Strain-Induced Precipitate Dissolution in an Irradiated Austenitic Alloy” *Scripta Mater.* 65 (2011) 159.

Z. Jiao and G.S. Was, “Segregation Behavior in Proton- and Heavy Ion-Irradiated Ferritic-Martensitic Alloys,” *Acta Mater.* 59 (2011) 4467-4481

Z. Jiao and G.S. Was, “Novel Features of Radiation-Induced Segregation and Radiation-Induced Precipitation in Austenitic Stainless Steels” *Acta Mater.* 59 (2011) 1220.

Z. Jiao and G.S. Was, “Impact of Localized Deformation on Irradiation-Assisted Stress Corrosion Cracking of Austenitic Stainless Steels”, *J. Nucl. Mater.* 408 (2011) 246.

Z. Jiao, G.S. Was, T. Miura; K. Fukuya, “Localized Deformation in Proton and Heavy Ion Irradiated Austenitic Stainless Steels”, TMS Annual Meeting, San Diego, CA, Feb. 27-Mar. 3, 2011.

Z. Jiao and G.S. Was, "Evolution of Radiation-induced Precipitates in Proton-irradiated HCM12A", TMS Annual Meeting, San Diego, CA, Feb. 27-Mar. 3, 2011.

Z. Jiao and G.S. Was, "APT Characterization of Radiation-induced Precipitation in Ferritic-Martensitic Alloys" TMS Annual Meeting, San Diego, CA, Feb. 27-Mar. 3, 2011.

L. Chen, Z. Jiao, L. Wang, G.S. Was, "Examination of Precipitates in T91 and HCM12A Alloy by the Replica Extraction Technique", TMS Annual Meeting, San Diego, CA, Feb. 27-Mar. 3, 2011.

Z. Jiao, G. S. Was, "Oxidation of a Proton-Irradiated 316 Stainless Steel in Simulated BWR NWC Environment," 15<sup>th</sup> Int'l. Conf. Environmental Degradation of Materials in Nuclear Power Systems – Water Reactors, J. T. Busby, G. Ilevbare, P. L. Andresen, Eds., John Wiley & Sons, Hoboken, New Jersey, 2011, 1329-1338.

O. Toader, "Fuzzy Logic Controls of a Particle Accelerator", 10-th European Workshop on Beam Diagnostics and Instrumentation for Particle Accelerators (DIPAC 2011), Hamburg, Germany, May 16-18 2011.

F.U. Naab, E.A. West, O.F. Toader, G.S. Was, "Conducting well-controlled ion irradiations to understand neutron irradiation effects in materials," AIP Conference Proceedings 1336, Application of Accelerators in Research and Industry, American Institute of Physics Press, New York (2011) 325-331.

V. Shankar and G. S. Was, "Proton Irradiation Creep of Beta-silicon Carbide," J. Nucl. Mater. 418 (2011) 198-206.

J. P. Wharry, Z. Jiao, V. Shankar, J. T. Busby, G. S. Was, "Radiation-induced Segregation and Phase Stability in Ferritic-Martensitic Alloy T91," J. Nucl. Mater. 417 (2011) 140-144.

G. S. Was, J. P. Wharry, B. Frisbie, B. D. Wirth, D. Morgan, J. D. Tucker and T. R. Allen, "Assessment of Radiation-Induced Segregation Mechanisms in Austenitic and Ferritic-Martensitic Alloys," J. Nucl. Mater. 411 (2011) 41-50.